FACULTY OF PHYSICS
UNIVERSITY OF WARSAW

Stability of electroweak vacuum and domain walls in extensions of the SM

Zygmunt Lalak
ITP Warsaw

with **M. Lewicki, P. Olszewski, T. Krajewski, O. Czerwińska** and **Ł. Nakonieczny**
arXiv:1402.3826 (JHEP), arXiv:1505.05505, arXiv:1605.06713 (PRD),
arXiv:1411.6435 (PRD), arXiv:1606.07808 (JHEP), arXiv:1508.03297 (JHEP)
arXiv:1608.05719 (JCAP), arXiv:1711.08473 [astro-ph.CO] (JHEP)

Corfu Summer Institute, September 2018

Outline:

- SM effective potential, tunneling and lifetime
- BSM physics via higher-order operators
- Modifications of due to expanding background and Coleman - De Luccia bounces
- SM + dilaton
- Domain walls
- Domain walls at finite temperature
- Domain walls and gravitational waves
- Summary

SM Effective potential

Standard Model Effective potential

$$V_{SM}(\mu) = -\frac{m^2}{2}\phi^2 + \frac{\lambda}{4}\phi^4 + \sum_i \frac{n_i}{64\pi^2} M_i^4 \left[\ln\left(\frac{M_i^2}{\mu^2}\right) - C_i \right]$$

For large field values $m^2 << \phi^2$ and $\mu = \phi$ the potential is very well approximated by

$$V_{SM}(\phi) \approx \phi^4 \left\{ \frac{\lambda}{4} + \frac{1}{64\pi^2} \left[6\left(\frac{g_2^2}{4}\right)^2 \left(\ln\left(\frac{g_2^2}{4}\right) - \frac{5}{6}\right) + 3\left(\frac{g_1^2+g_2^2}{4}\right)^2 \left(\ln\left(\frac{g_1^2+g_2^2}{4}\right) - \frac{5}{6}\right) \right.\right.$$
$$\left.\left. -12\left(\frac{y_t^2}{2}\right)^2 \left(\ln\left(\frac{y_t^2}{2}\right) - \frac{3}{2}\right) + \left(\frac{3\lambda}{2}\right)^2 \left(\ln\left(\frac{3\lambda}{2}\right) - \frac{3}{2}\right) + 3\left(\frac{\lambda}{2}\right)^2 \left(\ln\left(\frac{\lambda}{2}\right) - \frac{3}{2}\right) \right] \right\}$$

$$V_{SM}(\phi) \approx \frac{\lambda_{eff}(\phi)}{4}\phi^4$$

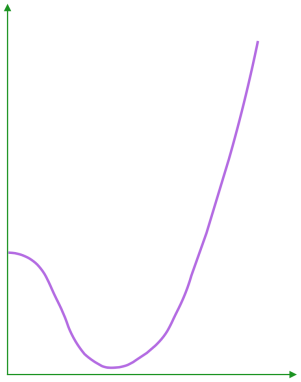

classically ← → quantum corrected ...

SM Metastability

$$\lambda_{eff} < 0 \Longrightarrow \text{Metastability}$$

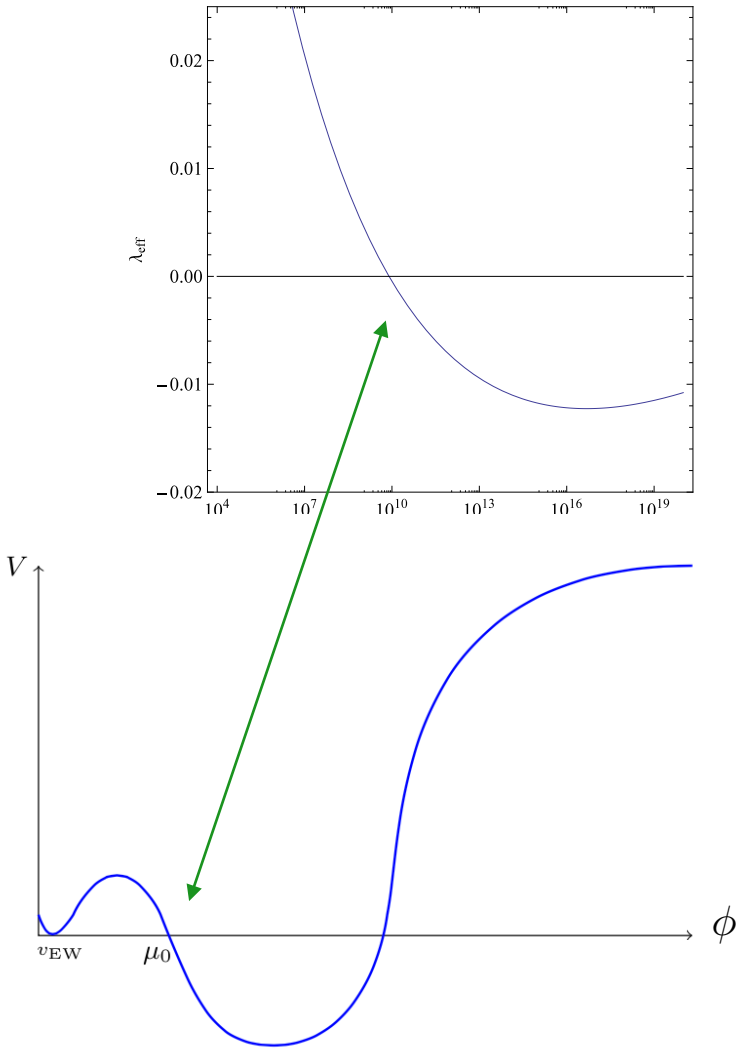

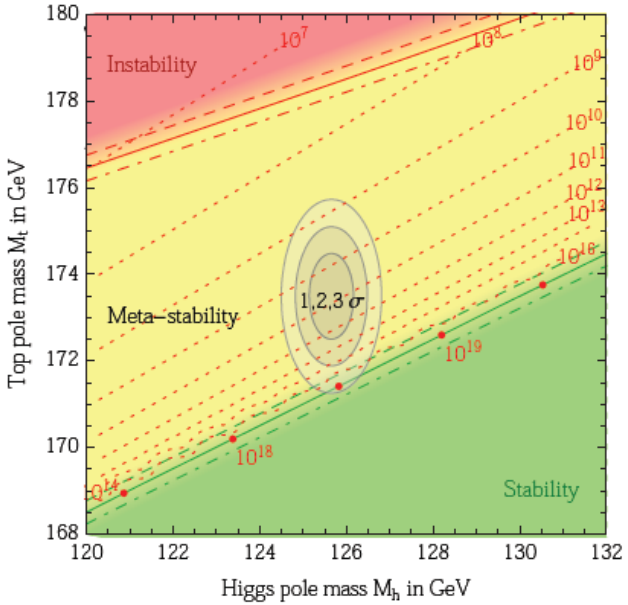

D. Buttazzo, et al. [arXiv:1307.3536].
G. Degrassi, et al. [arXiv:1205.6497].

See lectures by G. Degrassi Corfu 2014

Changes in the effective potential due to the changing top mass

$$m_{t\ phys} \approx \bar{m}_t + 10\,\mathrm{GeV}$$

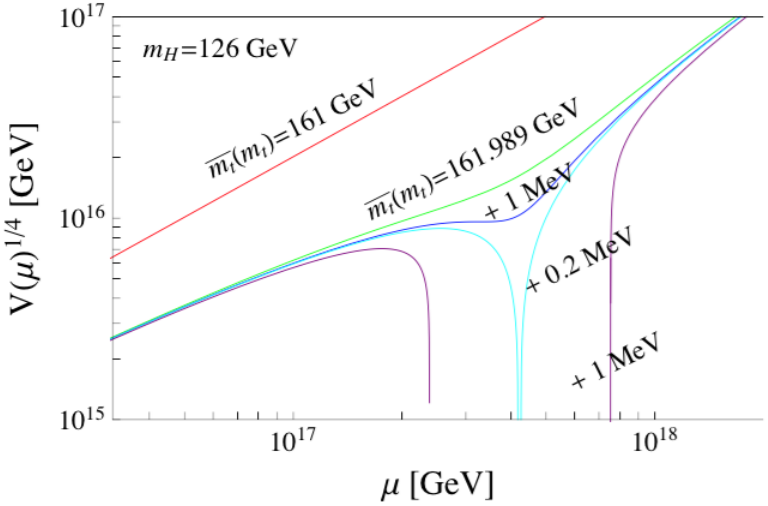

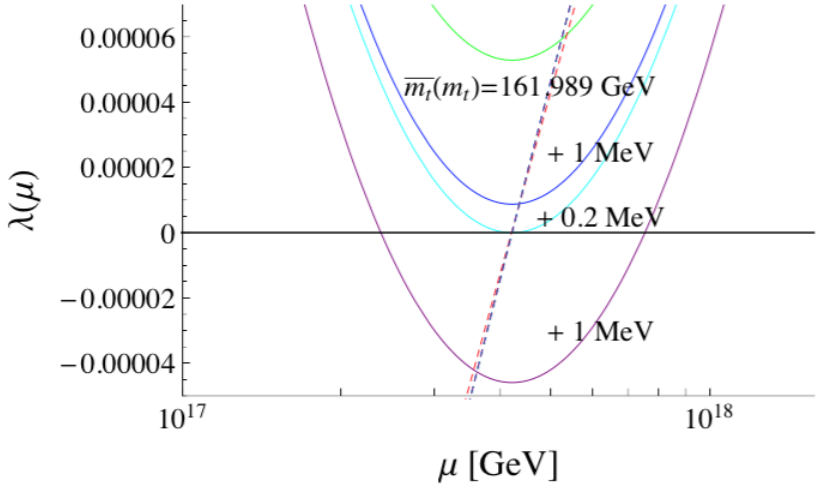

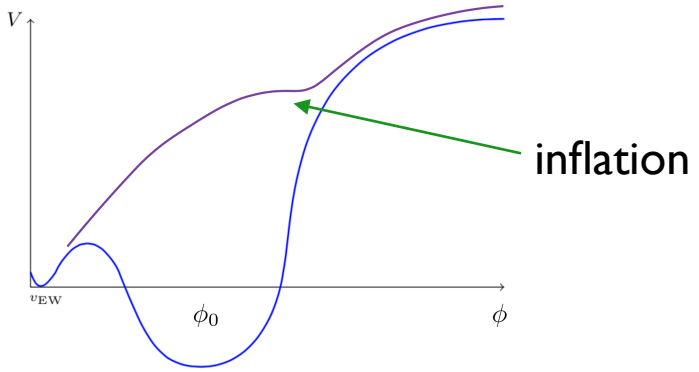

(I.Massina et al. 2013)

Tunneling

Standard semiclassical formalism

S. R. Coleman, Phys. Rev. D **15** (1977) 2929.
C. G. Callan, Jr. and S. R. Coleman, Phys. Rev. D **16** (1977) 1762.

$O(4)$ symmetric solution to euclidean equation of motion

$$\ddot{\phi} + \frac{3}{s}\dot{\phi} = \frac{\partial V(\phi)}{\partial \phi},$$
$$s = \sqrt{\vec{x}^2 + x_4^2}.$$

with

- $\dot{\phi}(s = 0) = 0$ near the true vacuum
- $\phi(s = \infty) = \phi_{min}$ at the false vacuum
  $= v_{EW}$

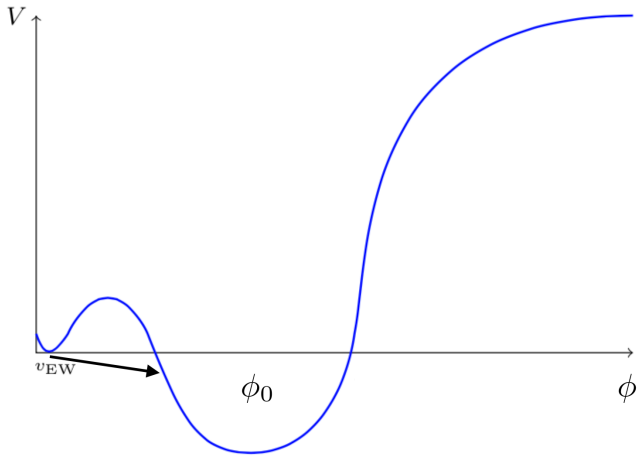

Tunneling

Action of the bounce solution

$$\begin{aligned} S_E &= \int d^4x \left\{ \frac{1}{2} \sum_{\alpha=1}^{4} \left(\frac{\partial \phi(\mathbf{x})}{\partial x^\alpha} \right)^2 + V(\phi(\mathbf{x})) \right\} \\ &= 2\pi^2 \int ds s^3 \left(\frac{1}{2} \dot{\phi}^2(s) + V(\phi(s)) \right), \end{aligned}$$

allows us to calculate decay probability dp of a volume d^3x

$$dp = dt d^3x \frac{S_E^2}{4\pi^2} \left| \frac{det'[-\partial^2 + V''(\phi)]}{det[-\partial^2 + V''(\phi_0)]} \right|^{-1/2} e^{-S_E}.$$

Simplifying

- normalisation factor replaced with width of the barrier $\propto \phi_0$
- size of the universe is $T_U = 10^{10}$yr

we can calculate the lifetime of the false vacuum ($p(\tau) = 1$)

$$\frac{\tau}{T_U} = \frac{1}{\phi_0^4 T_U^4} e^{S_E}.$$

Standard Model

Approximating by a quartic potential:

$$\frac{\tau}{T_U} = \frac{1}{\phi^4(\lambda_{min})\, T_U^4} e^{\frac{8\pi^2}{3|\lambda_{min}|}} \approx 10^{540}.$$

lifetime is minimal for ϕ that minimizes $\lambda_{eff}(\phi)$.

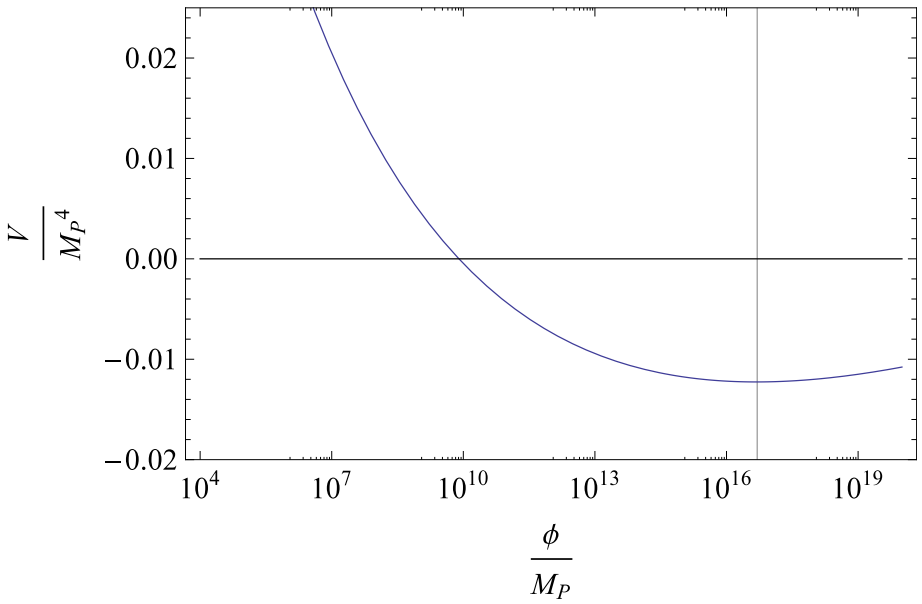

New extrema created by quantum corrections
(Coleman-Weinberg mechanism)

condition for cancellation of corrections to the derivative of SM

$$\lambda = \frac{\hbar}{256\pi^2}\left[g_1^4 + 2g_1^2 g_2^2 + 3g_2^4 - 48h_t^4 - 3(g_1^2+g_2^2)^2 \log\frac{g_1^2+g_2^2}{4} - 6g_2^4 \log\frac{g_2^2}{4} + 48y_t^4 \log\frac{y_t^2}{2}\right]$$

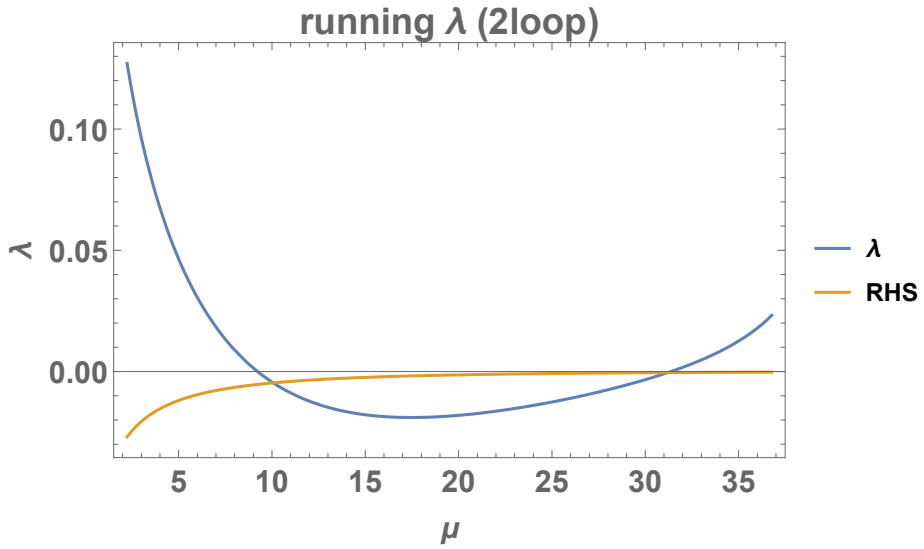

Hence sensitivity to New Physics

Effective potential with nonrenormalisable interactions

We add new nonrenormalisable couplings
(similar to V. Branchina and E. Messina, [arXiv:1307.5193].)

$$V \approx \frac{\lambda_{eff}(\phi)}{4}\phi^4 + \frac{\lambda_6}{6!}\frac{\phi^6}{M_p^2} + \frac{\lambda_8}{8!}\frac{\phi^8}{M_p^4}.$$

New Physics at Planck scale

That modify the potential around the Planck scale:

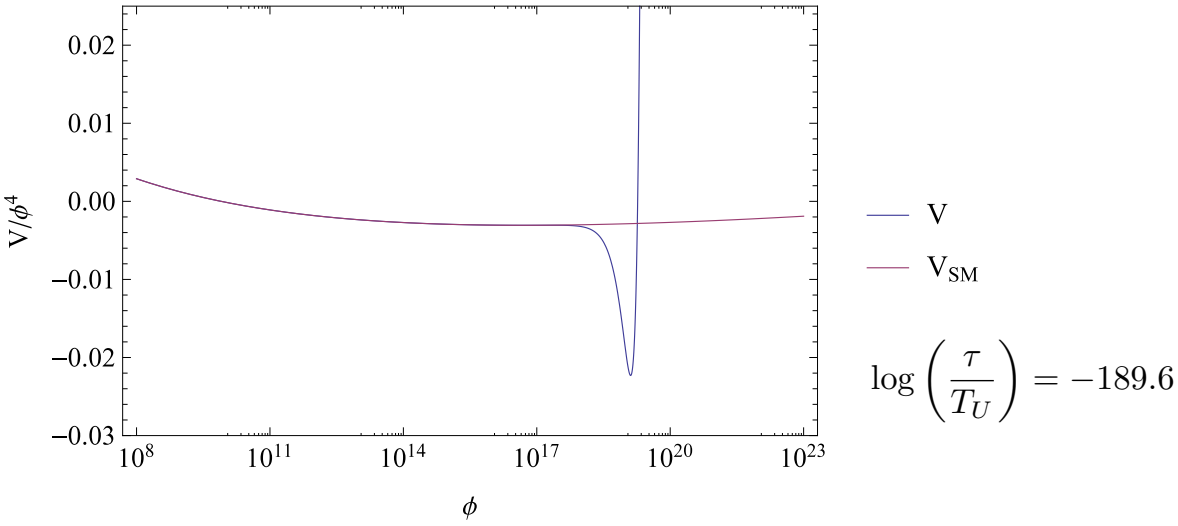

Figure: effective potential with $\lambda_6 = -1$ and $\lambda_8 = 1$.

Numerical vs Analytical again

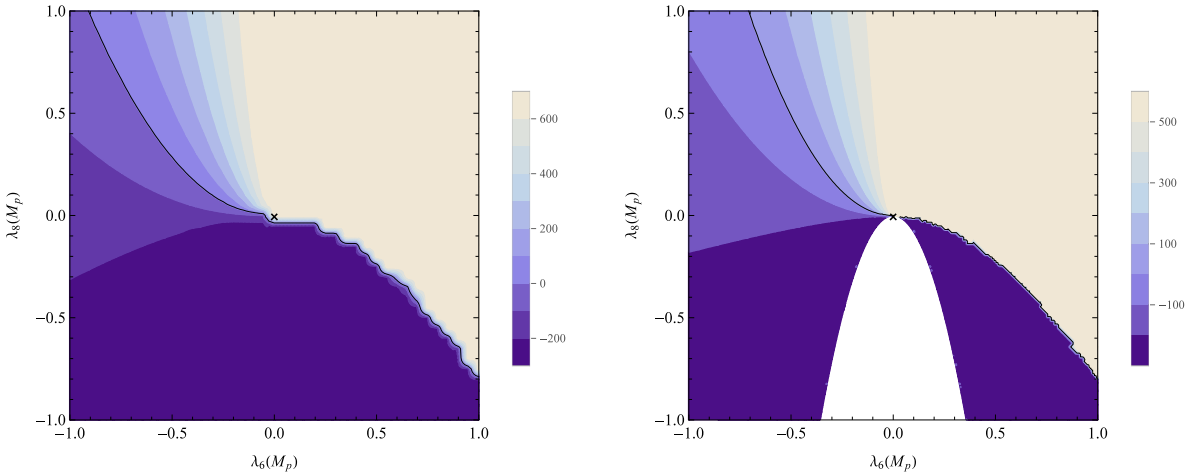

Figure: Decimal logatihm of lifetime of the universe in units of T_U as a function of the nonrenormalisable $\lambda_6(M_p)$ and $\lambda_8(M_p)$ couplings, calculated numerically (left panel) and analytically (right panel).

Magnitude of the suppression scale

Approximate lifetime:

$$\frac{\tau}{T_U} = \frac{1}{\mu^4(\lambda_{min})\, T_U^4} e^{\frac{8\pi^2}{3|\lambda_{min}|}}.$$

Positive λ_6 and $\lambda_8 \rightarrow$ stabilizing the potential

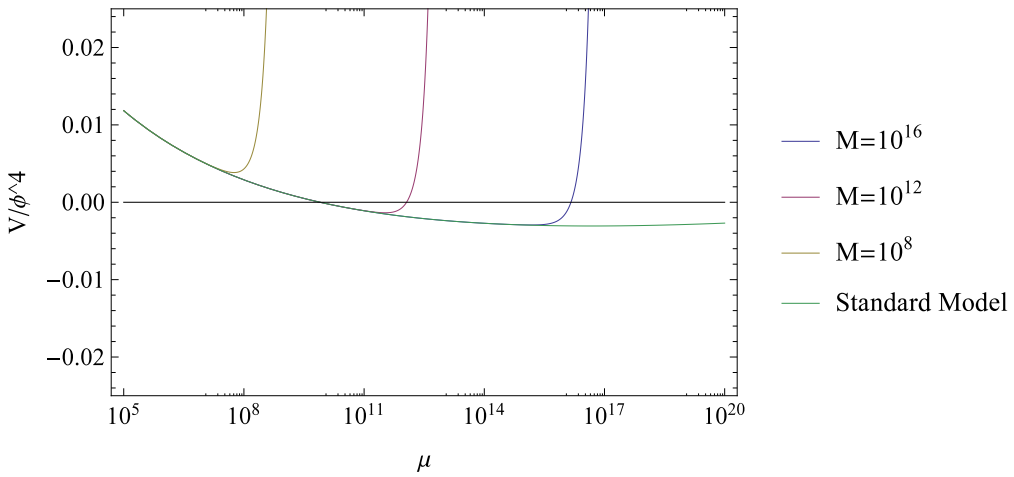

Figure: Scale dependence of $\frac{\lambda_{eff}}{4} = \frac{V}{\phi^4}$ with $\lambda_6 = \lambda_8 = 1$ for different values of suppression scale M. The lifetimes corresponding to suppression scales $M = 10^8, 10^{12}, 10^{16}$ are, respectively, $\log_{10}(\frac{\tau}{T_U}) = \infty, 1302, 581$ while for the Standard Model $\log_{10}(\frac{\tau}{T_U}) = 540$.

Magnitude of the suppression scale

Positive λ_8 and negative $\lambda_6 \rightarrow$ New Minimum

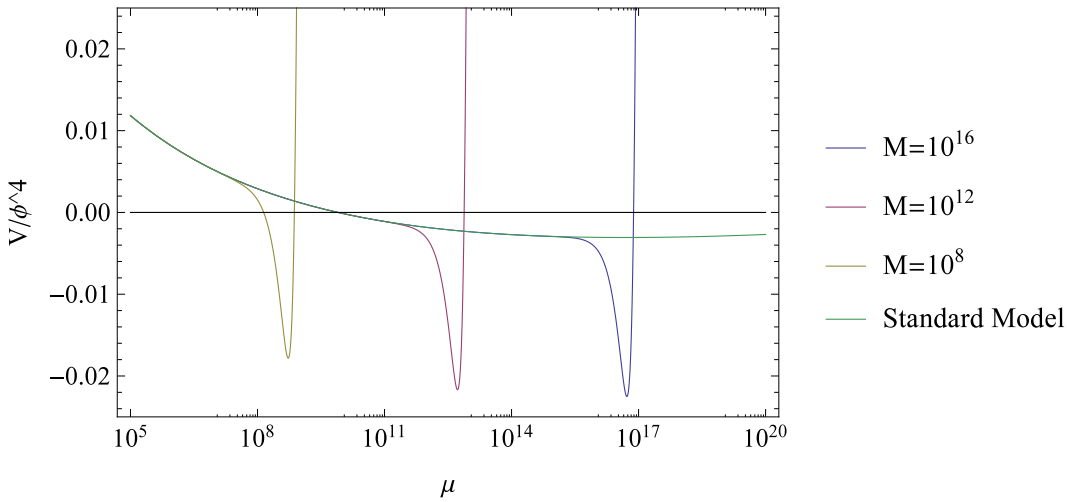

Figure: Scale dependence of $\frac{\lambda_{eff}}{4} = \frac{V}{\phi^4}$ with $\lambda_6 = -1$ and $\lambda_8 = 1$ for different values of suppression scale M. The lifetimes corresponding to suppression scales $M = 10^8, 10^{12}, 10^{16}$, are, respectively, $\log_{10}(\frac{\tau}{T_U}) = -45, -90, -110$ while for the Standard Model $\log_{10}(\frac{\tau}{T_U}) = 540$.

SM + dilaton

Additional singlet scalar

$$\mathcal{L} = \frac{1}{2}(\partial h)^2 + \frac{1}{2}(\partial S)^2 - \frac{m^2}{2}h^2 - \frac{M^2}{2}S^2 + \frac{\lambda_{hS}}{4}h^2S^2 + \frac{\lambda}{4}h^4 + + \frac{\lambda_S}{4}S^4$$

$$\lambda' = \frac{1}{4\pi^2}\left(24\lambda^2 - 6y_t^4 + 12\lambda y_t^2 + \lambda_{hS}^2 + \frac{9}{8}g_2^4 + \frac{3}{8}g_1^4 + \frac{3}{4}g_2^2 g_1^2 - 9\lambda g_2^2 - 3\lambda g_1^2\right)$$

$$\lambda_S' = \frac{1}{4\pi^2}\left(10 * \lambda_S^2 + \lambda_{hX}^2\right)$$

$$\lambda_{hS}' = \frac{\lambda_{hS}}{4\pi^2}\left((2\lambda_{hS} + 6\lambda + 4\lambda_S + 3y_t^2 - \frac{9}{4}g_2^2 - \frac{3}{4}g_1^2\right)$$

$$- \mathcal{M}^2 = \begin{pmatrix} -m^2 + 3\lambda v_0^2 & \lambda_{hS} v_0 v_S \\ \lambda_{hS} v_0 v_S & -M^2 + 3\lambda_S v_S \end{pmatrix}$$

$$v_S^2 = v_0^2 / \tan^2\beta \qquad\qquad m_h = 125.09\text{GeV}$$

Additional singlet scalar

$$\mathcal{L} = \frac{1}{2}(\partial h)^2 + \frac{1}{2}(\partial S)^2 - \frac{m^2}{2}h^2 - \frac{M^2}{2}S^2 + \frac{\lambda_{hS}}{4}h^2S^2 + \frac{\lambda}{4}h^4 + + \frac{\lambda_S}{4}S^4$$

$$\lambda' = \frac{1}{4\pi^2}\left(24\lambda^2 - 6y_t^4 + 12\lambda y_t^2 + \lambda_{hS}^2 + \frac{9}{8}g_2^4 + \frac{3}{8}g_1^4 + \frac{3}{4}g_2^2g_1^2 - 9\lambda g_2^2 - 3\lambda g_1^2\right)$$

$$\lambda_S' = \frac{1}{4\pi^2}\left(10 * \lambda_S^2 + \lambda_{hX}^2\right)$$

$$\lambda_{hS}' = \frac{\lambda_{hS}}{4\pi^2}\left((2\lambda_{hS} + 6\lambda + 4\lambda_S + 3y_t^2 - \frac{9}{4}g_2^2 - \frac{3}{4}g_1^2\right)$$

$$- \mathcal{M}^2 = \begin{pmatrix} -m^2 + 3\lambda v_0^2 & \lambda_{hS} v_0 v_S \\ \lambda_{hS} v_0 v_S & -M^2 + 3\lambda_S v_S \end{pmatrix}$$

$$v_S^2 = v_0^2 / \tan^2\beta \qquad m_h = 125.09\text{GeV}$$

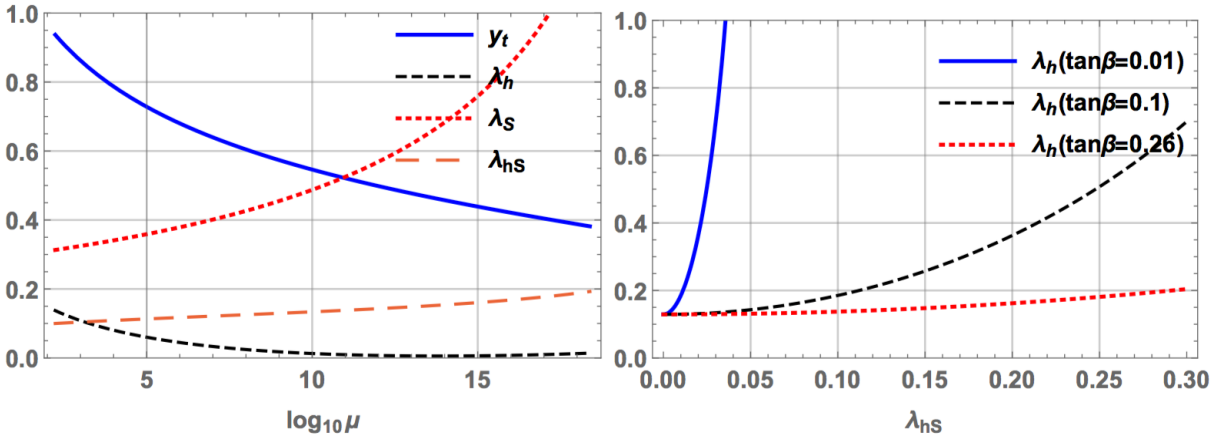

FIG. 1: Left panel shows an example of running of λs in our model. Right panel shows Higgs λ as a function of λ_{hS}.

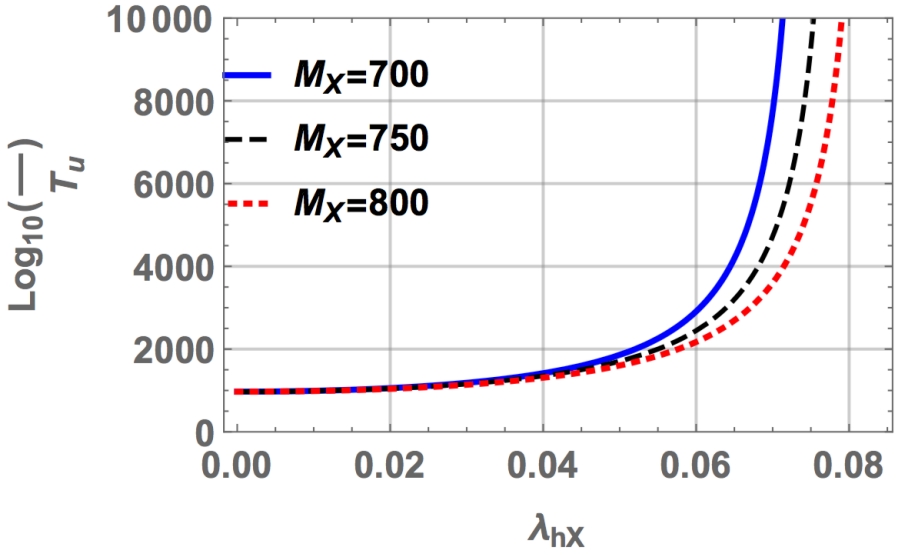

FIG. 2: lifetime of the vacuum as a function of λ_{hS}.

Integrating the scalar out

$\mathbb{Z}^2$ symmetry: $(\varphi, \Phi) \to (-\varphi, -\Phi)$

$$\mathcal{L}(\varphi, \Phi) = \frac{1}{2}(\partial\varphi) + \frac{1}{2}(\partial\Phi) - V(\varphi, \Phi)$$

$$V(\varphi, \Phi) = -\frac{1}{2}m^2\varphi^2 + \frac{1}{2}M^2\Phi^2 + V^{(4)}(\varphi, \Phi)$$

$$V^{(4)}(\varphi, \Phi) = \frac{\lambda}{4}\varphi^4 + \xi\varphi^3\Phi + \frac{\kappa}{2}\varphi^2\Phi^2 + \frac{\rho}{3}\varphi\Phi^3 + \frac{\theta}{4}\Phi^4$$

$$\mathcal{L}_{\text{eff}}(\varphi) = \frac{1}{2}K(\varphi)(\partial\varphi)^2 - V(\varphi) + \mathcal{O}(\partial^4)$$

$$0 = \left.\frac{\delta\mathcal{L}}{\delta\Phi}\right|_{\Phi=\Phi^{\text{EOM}}(\varphi)}$$

$$\mathcal{L}_{\text{eff}}(\varphi) = \mathcal{L}(\varphi, \Phi^{\text{EOM}}(\varphi)) + \mathcal{O}^2(\hbar)$$

$$\Phi^{\mathrm{EOM}}(\varphi)=-\xi\frac{\varphi^3}{\Delta}+\xi\frac{1}{\Delta}\left(\Box\frac{\varphi^2}{\Delta}\right)-\xi^2\rho\frac{\varphi^7}{\Delta^3}+\xi^3\theta\frac{\varphi^9}{\Delta^4}+\mathcal{O}^2\left(\rho,\theta,\frac{\Box}{M^2}\right),\quad \Delta\equiv M^2+\kappa\varphi^2$$

$$K(\varphi)=1+\left(-3\frac{\xi\varphi^2}{\Delta}+2\frac{\kappa\xi\varphi^4}{\Delta^2}\right)^2$$

$$V(\phi)=-\frac{m^2}{2}\varphi^2+\frac{\lambda}{4}\varphi^4-\frac{\xi^2}{2}\frac{\varphi^6}{\Delta}-\frac{\rho\xi^3}{3}\frac{\varphi^{10}}{\Delta^3}+\frac{\theta\xi^4}{4}\frac{\varphi^{12}}{\Delta^4}+\mathcal{O}^{(2)}(\rho,\theta)$$

$$\ddot{\varphi}_B+\frac{3}{s}\dot{\varphi}_B+\frac{K'}{2K}\left(\dot{\varphi}\right)^2-\frac{V'}{K}=0$$

$$S_{\mathrm{eff}}\equiv 2\pi^2\int s^3\mathrm{d}s\left[\frac{1}{2}K(\varphi_B)\left(\dot{\varphi}_B\right)^2+V(\varphi_B)\right]$$

$$\varphi_{\mathrm{eff}}(\varphi)\equiv\int_0^{\varphi}\sqrt{K(\varphi')}\mathrm{d}\varphi'\approx\varphi+\frac{9}{10}\xi^2\frac{\varphi^5}{M^4}-\frac{15}{7}\kappa\xi^2\frac{\varphi^7}{M^6}$$

$$\varphi(\varphi_{\mathrm{eff}})\approx\varphi_{\mathrm{eff}}-\frac{9}{10}\xi^2\frac{\varphi_{\mathrm{eff}}^5}{M^4}+\frac{15}{7}\kappa\xi^2\frac{\varphi_{\mathrm{eff}}^7}{M^6}$$

$$\frac{1}{2}\left(\partial\varphi_{\mathrm{eff}}\right)^2=\frac{1}{2}\left[K(\varphi)+\mathcal{O}\left(\frac{\varphi^8}{M^8}\right)\right](\partial\varphi)^2$$

$$\begin{aligned}\widetilde{V}(\varphi_{\mathrm{eff}})&\equiv V(\varphi(\varphi_{\mathrm{eff}}))\\&=-\frac{m^2}{2}\varphi_{\mathrm{eff}}^2+\frac{\lambda}{4}\varphi_{\mathrm{eff}}^4-\left(\frac{1}{2}-\frac{9}{10}\frac{m^2}{M^2}\right)\xi^2\frac{\varphi_{\mathrm{eff}}^6}{M^2}\\&+\left(-\frac{15}{7}\frac{m^2}{M^2}\kappa+\frac{1}{2}\kappa-\frac{63}{70}\lambda\right)\xi^2\frac{\varphi_{\mathrm{eff}}^8}{M^4}+\mathcal{O}\left(\frac{\varphi_{\mathrm{eff}}^{10}}{M^6}\right)\end{aligned}$$

$$\mathcal{L}_{\mathrm{eff}}^{(8)}(\varphi)\equiv\frac{1}{2}\left(\partial\varphi\right)^2-\widetilde{V}(\varphi)$$

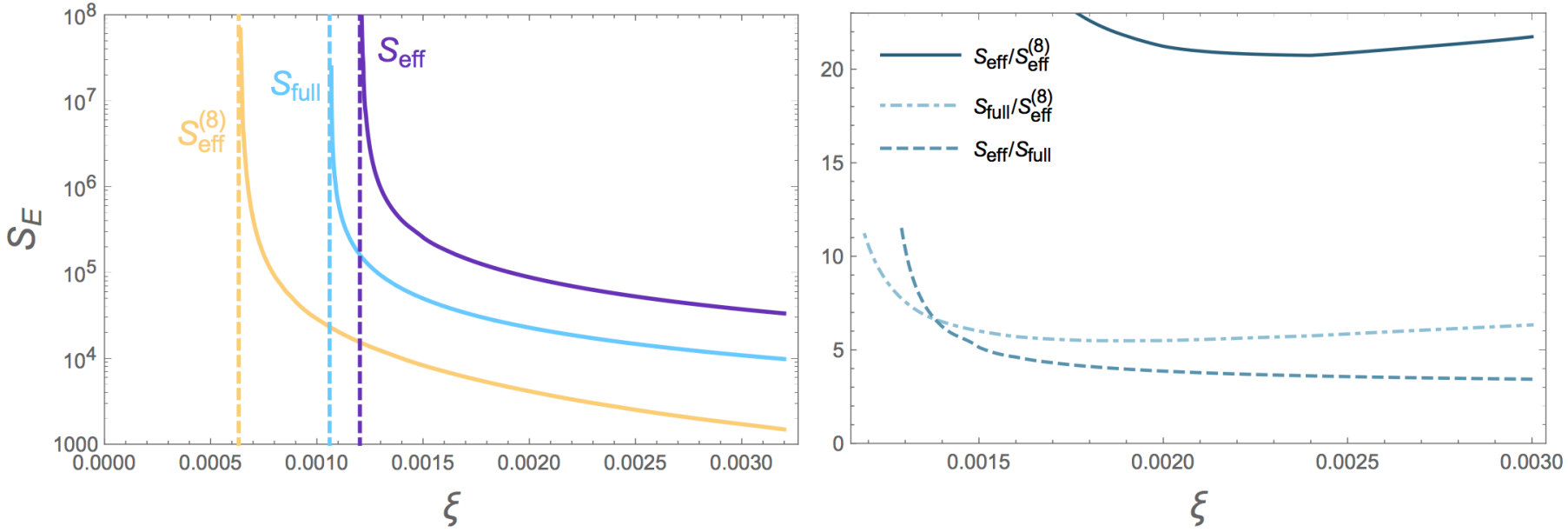

Figure 1.9: Left: Action of the euclidean tunneling bounce configurations S_{full}, S_{eff}, $S_{\text{eff}}^{(8)}$, obtained from the respective Lagrangians $\mathcal{L}(\varphi, \Phi)$, $\mathcal{L}_{\text{eff}}(\varphi)$, $\mathcal{L}_{\text{eff}}^{(8)}(\varphi)$ for values of parameters specified in (2.68). Notice the logarithmic vertical scale. Right: Ratios of the actions plotted on the left.

$$M = 10^3\, m$$
$$\lambda = 10^{-3}\,, \quad \kappa = 2\times 10^{-3}\,, \quad \rho = 10^{-3}\,, \quad \theta = 6\times 10^{-3}$$
$$\xi \in [0;3]\times 10^{-3}$$

Quantum scale symmetric effective lagrangian

See talks by G.G. Ross and D. Ghilencea

No scale anomaly in

„*dynamical*" *regulator*

$$\mathcal{L}^{(0)}(\phi,\sigma) = \frac{1}{2}(\partial\phi)^2 + \frac{1}{2}(\partial\sigma)^2 - \mu^{2\varepsilon}(\sigma)\left[\underbrace{V(\phi,\sigma)}_{\text{renormalizable, classicaly scale-invariant}} + \sum_{n=0}\lambda_n\frac{\phi^{4+2n}}{\sigma^{2n}}\right]$$

$\mathbb{Z}^2 \times \mathbb{Z}^2$

$\phi \to -\phi$

$\sigma \to -\sigma$

go to *broken phase*

$$\mathcal{L}^{(0)}(\phi_0+\phi', \sigma_0+\phi')$$

compute loop corrections (in momentum expansion) & RGE functions *β, γ*

$$\mathcal{L}_{\text{eff}}(\phi,\sigma) = -V_{\text{eff}}(\phi,\sigma) + \ldots$$

- Homogenous function (no mass-parameters, only vev's)
- $\mathbb{Z}^2 \times \mathbb{Z}^2$ sym.
- Satisfies Callan-Symanzik eq.

Quantum scale symmetric effective lagrangian

RG-improvement:

$$\mu = e^t \mu_0 \,, \qquad \lambda(t)\,\phi^4 + \frac{\lambda^2(t)\phi^4}{64\pi^2}\,\log\left(\frac{\phi}{e^t\sigma}\right)^2 + \ldots$$

Choose $t = t(\phi,\sigma) \sim \log\frac{\phi}{\sigma}$ to avoid large logs.

Spontanous scale-symmetry breaking:

$$\begin{pmatrix}\phi\\ \sigma\end{pmatrix} = M\begin{pmatrix}\sin\theta\\ \cos\theta\end{pmatrix}\,, \quad V_{\rm eff} = M^4\,W(\theta)\,,$$

→ flat direction in $V_{\rm eff}$ $\Rightarrow$

$$\exists_{\theta=\theta_0}\, W(\theta_0) = W'(\theta_0) = 0$$

renormalization condition, similar to choosing C.C.

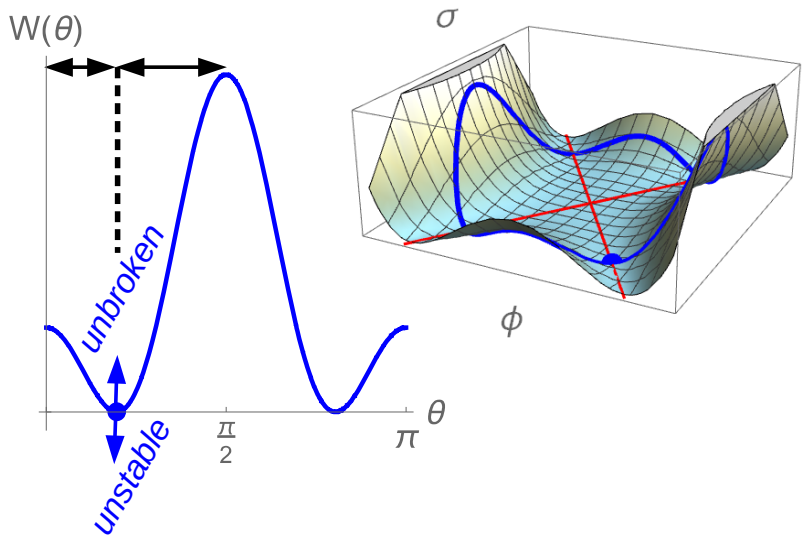

- **Hierarchy** of scales via **aligning** the flat direction $\perp\phi$ → $\theta_0 \approx \frac{\phi_0}{\sigma_0} \ll 1$
- New perspective on **naturalness**: is this alignement stable wrt. embedding in a UV completion?

Quantum scale symmetric SM + σ

$$H = \begin{pmatrix} 0 \\ \frac{\phi}{\sqrt{2}} \end{pmatrix}$$

(electroweak vacuum → electroweak flat direction)

$$\mathcal{L}_{SM}\Big|_{\substack{m^2=0 \\ \mu=\mu(\sigma)}} + \frac{1}{2}(\partial\sigma)^2 - \lambda_m |H|^2\sigma^2 - \frac{\lambda_\sigma}{4}\sigma^4 + \sum_{n=0}\lambda_n \frac{|H|^{4+2n}}{\sigma^{2n}}$$

$$V_{\rm eff}^{\rm SM}(\phi,\sigma) \approx \frac{1}{4}\lambda_{\rm eff}\left(\log\frac{\phi}{\sigma}\right)\phi^4 = M^4 \underbrace{\lambda_{\rm eff}(\log\tan\theta)\frac{\tan^4\theta}{(1+\tan^2\theta)^2}}_{W(\theta)}$$

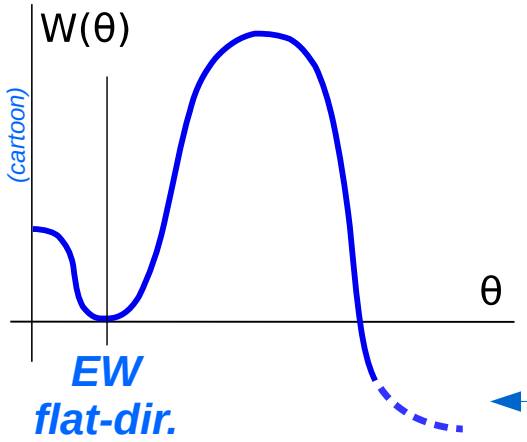

$V_{\rm eff}$ is:

- ***unstable***
- ***unbounded below***

Tunneling via **2-dim instanton** (Coleman's bounce), in the presence of nonrerm. terms.

(Even stronger) motivation to stabilise the ***$V_{\rm eff}$*** completely: $\lambda_{\rm eff} \overset{!}{>} 0$

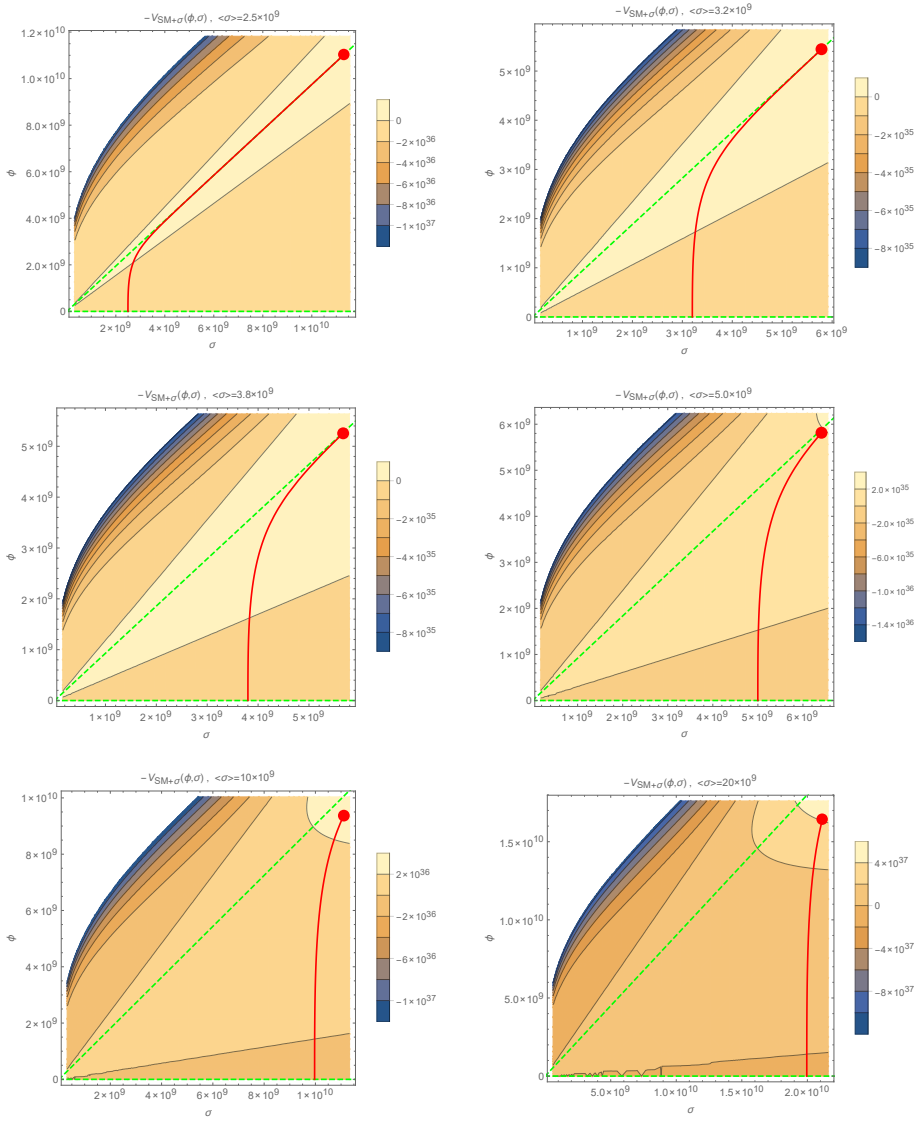

FIG. 2. Contour plots of the effective potentials $-V_{SM+\sigma}(\phi,\sigma)$ for various choices of $\langle\sigma\rangle$. Lower green dashed line marks the electroweak vacuum-direction, higher green dashed line marks the direction of greatest instability. Red continuous line is a plot of the bounce configuration (ϕ_B,σ_B). (Note that, mainly due to varying contribution of the nonrenormalizable interaction from one plot to another, the plots present differing potentials and it would be misleading to plot the bounce configurations in a single frame.)

$M_s[GeV]$	$\lambda_6(0)$	$S_B^{SM+\sigma}$	$S_B^{SM+\lambda_6}$
2.5×10^9	1.7×10^{-4}	1.18×10^6	4.38×10^6
3.2×10^9	2.2×10^{-4}	1.77×10^5	2.24×10^5
3.8×10^9	2.5×10^{-4}	9.13×10^4	1.02×10^5
5×10^9	3.0×10^{-4}	4.62×10^4	4.82×10^4
1×10^{10}	4.2×10^{-4}	1.83×10^4	1.85×10^4
2×10^{10}	5.3×10^{-4}	1.10×10^4	1.11×10^4

TABLE I. Action of tunneling bounce configurations found in the two described setups for six increasing values of $M_s = \langle\sigma\rangle = \Lambda$. This value has a different meaning in the two models. In $SM{+}\lambda_6$ it is simultaneously the suppression scale Λ in the ϕ^6 interaction and location of the global minimum (*true vacuum*), $M_s = \langle\phi\rangle_{tv}$. In $SM{+}\sigma$ it is the VEV of σ in the electroweak vacuum ray, $M_s = \langle\sigma\rangle$. The low scale physics described by the models is the same but the electroweak vacuum is less stable in $SM{+}\sigma$ for values of M_s only slightly above the instability scale.

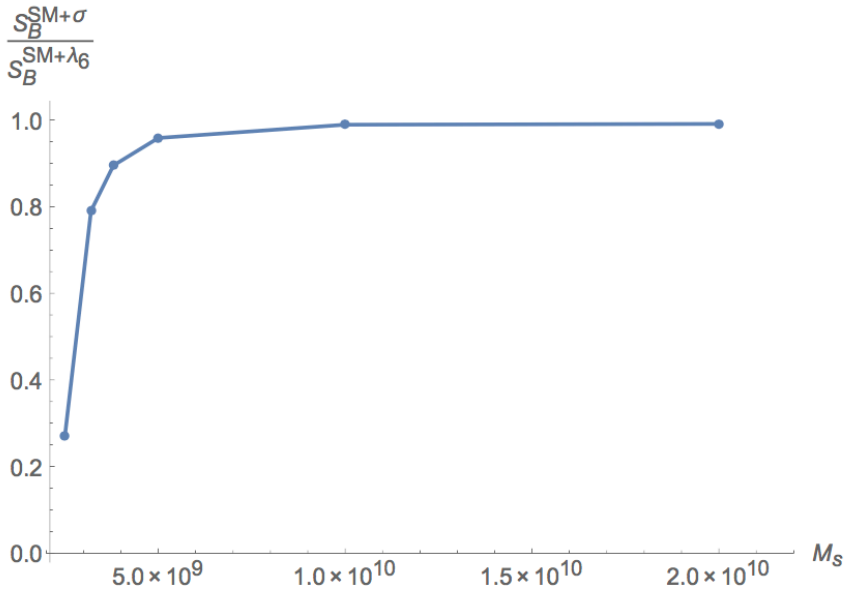

FIG. 3. Ratio of bounce's actions in the two discussed models. When potential in the unstable region becomes dominated by the new ϕ^6 term, there is a discrepancy between the two values of S_B. Compare with FIG. 1. and TABLE I. Note that the value M_S has slightly different meanings in the two setups.

Summary

SM + dilaton

1) You may use **a field as the scale *μ***
in Dim-Reg to preserve scale symmetry at the quantum level.

2) The price to pay: infinitely many nonpolynomial ϕ/σ operators
and corresponding couplings: **nonrenormalizability**.

3) Minimal subtraction scheme involves **evanescent interactions**.

4) Presence of a **flat direction** $\leftarrow$ tuning.

5) **Naturalness: aligning** the flat direction perpendicular to Higgs

6) **Instability = unboundedness below**

Gravity Corrections in Curved Space

Large field region

Stability in RD

$$V(h^4) = \frac{\lambda_{eff}(h)}{4} h^4 + V^{(1)}_{grav}$$

$$b = \frac{y_t^2 h_0^2}{2}$$

$$V(h^4) = \frac{\lambda_{eff}(h)}{4} h^4 + \frac{1}{64\pi^2}\frac{4}{3} R_{\alpha\beta\mu\nu} R^{\alpha\beta\mu\nu} \ln\left(\frac{b}{\mu^2}\right) =$$

$$= \frac{1}{4}\left[\lambda_{eff}(h) + \frac{4}{64\pi^2}\frac{4}{3}\frac{8}{3}\left(\bar{M}_P^{-2}\rho\right)^2 \frac{\tilde{c}}{h^4}\right]_{|h=h_0} h^4 = \frac{1}{4}\bar{\lambda}_{eff}(h) h^4$$

$$\bar{\lambda}_{eff}(\rho, h_0) = 0 \ ?$$

For $h_0 = 10^{10}\,\mathrm{GeV}$ and $\lambda_{off} = -0.02$ one obtain the scale $\nu \approx 10^{14}\,\mathrm{GeV}$

Stability in dS

$$V(h^4) = \frac{1}{4}\left[\lambda_{eff}(h) - 2\xi_h \frac{R}{h^2}\right]_{|h=h_0} h^4$$

$$\bar{\lambda}_{eff}(\rho, h_0) = 0 \ ? \quad \Rightarrow \quad \nu \sim 7 \cdot 10^{13}\,\mathrm{GeV}$$

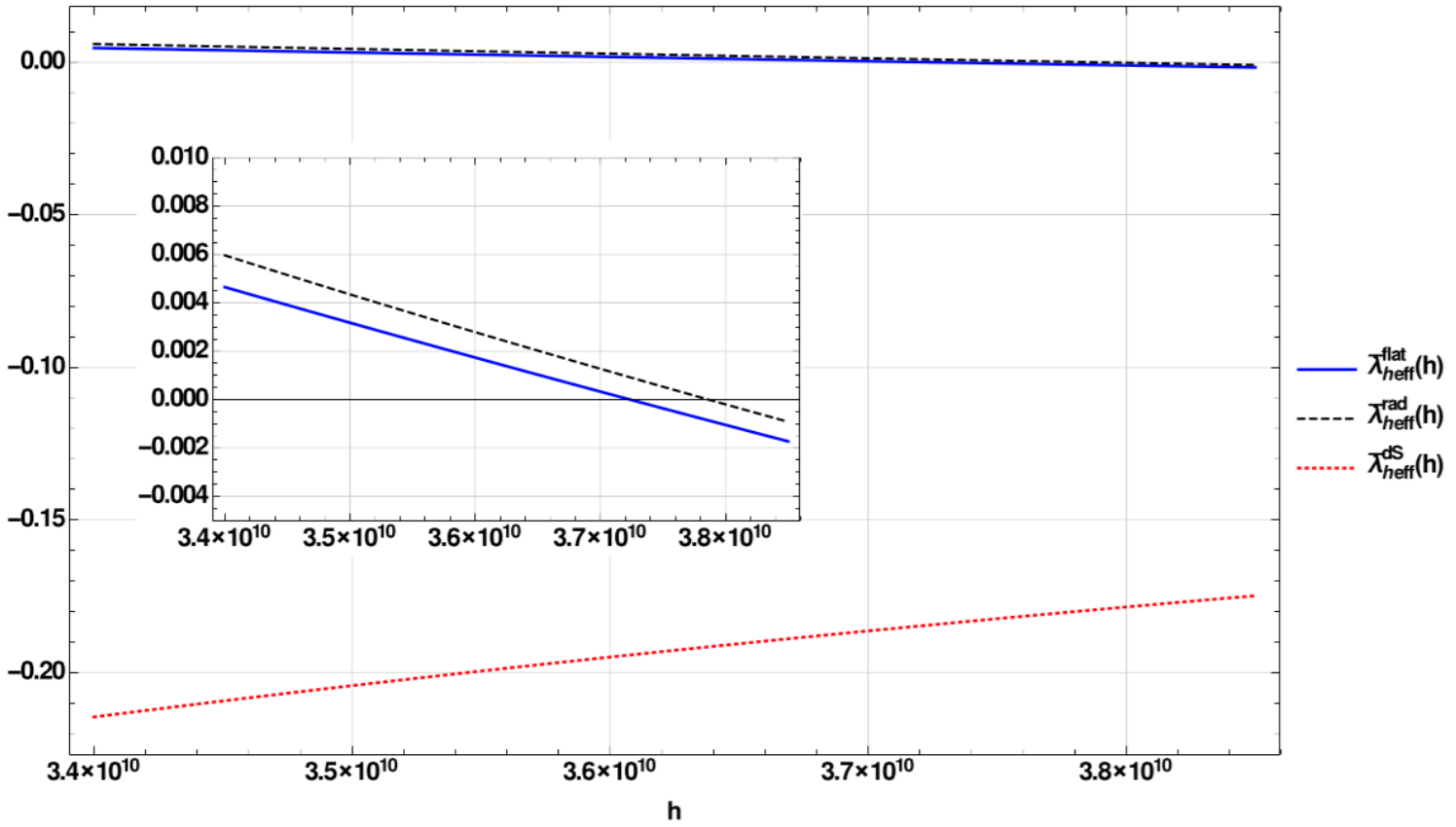

Figure 10: The effective quartic Higgs coupling, as defined by the relation $\bar{\lambda}_{heff}(h) \equiv \frac{4V^{(1)}(h)}{h^4}$, for various equations of state: $flat$ – flat spacetime result, rad – radiation dominance ($p = \frac{1}{3}\rho$), dS – de Sitter like ($p = -\rho$). The energy density was given by $\rho = \rho_{hc} + (\frac{y_t h}{\sqrt{2}})^4$, where ρ_{hc} was specified by the relation (4.36) and equal to $\rho_{hc} = (2.04 \cdot 10^{14} GeV)^4$. The X field was constant and set as equal to $X = v_X$. The non-minimal couplings were $\xi_h = \xi_X = 0$ at the $\mu = m_t$. The insert shows a close up of the difference for the flat spacetime and the radiation dominated era.

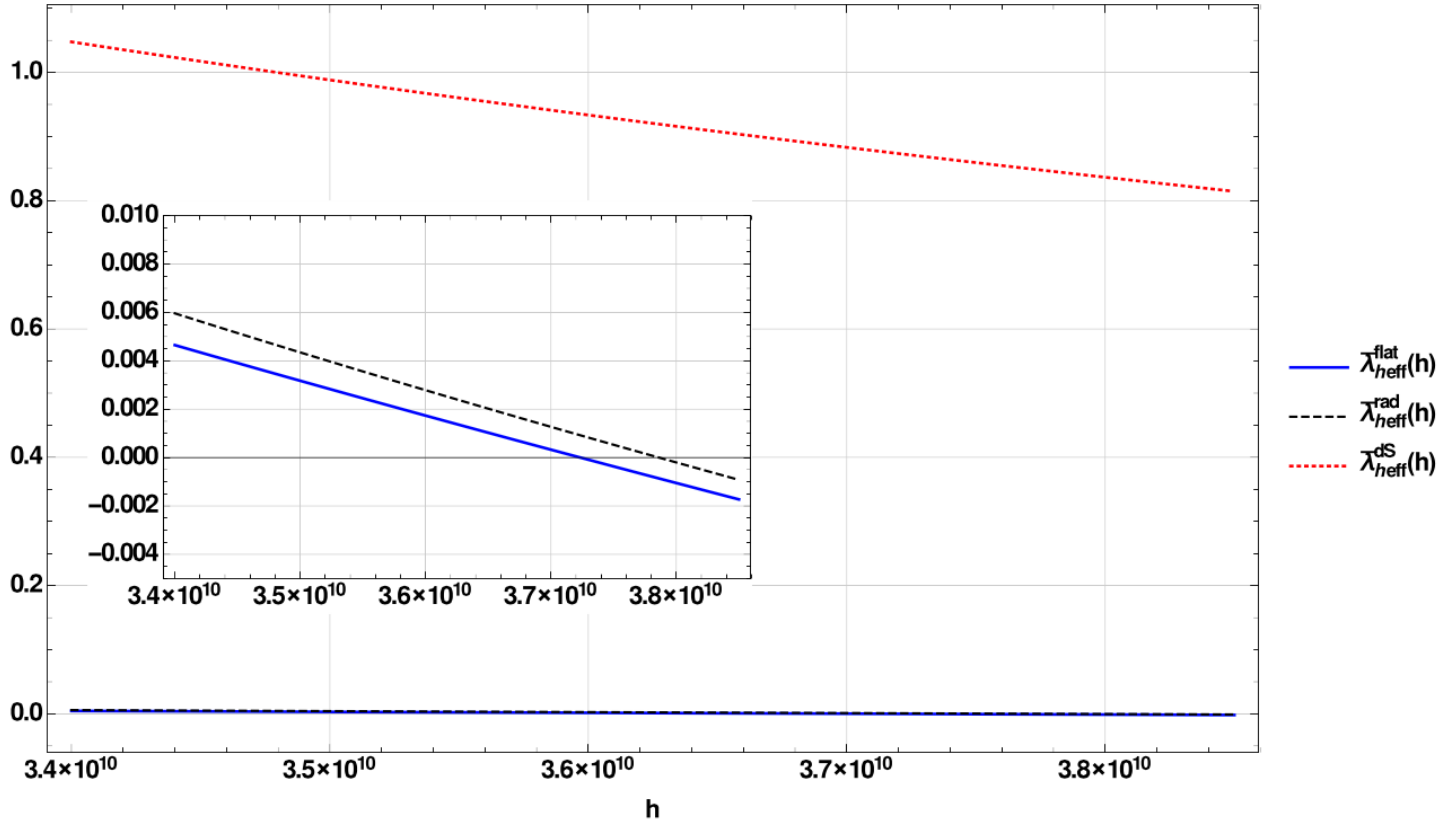

Figure 11: The effective quartic Higgs coupling, as defined by the relation $\bar{\lambda}_{heff}(h) \equiv \frac{4V^{(1)}(h)}{h^4}$, for various equations of state: $flat$ – flat spacetime result, rad – radiation dominance ($p = \frac{1}{3}\rho$), dS – de Sitter like ($p = -\rho$). The energy density was given by $\rho = \rho_{hc} + (\frac{y_t h}{\sqrt{2}})^4$, where ρ_{hc} was specified by the relation (4.36) and equal to $\rho_{hc} = (2.04 \cdot 10^{14} GeV)^4$. The X field was constant and set as equal to $X = v_X$. The non-minimal couplings were $\xi_h = \xi_X = \frac{1}{3}$ at the $\mu = m_t$. The insert shows a close up of the difference for the flat spacetime and the radiation dominated era.

Coleman-De Luccia bounces

$$\mathcal{L} = \frac{1}{2}(\partial\phi)^2 - V, \quad V = -a^2(3b-1)\phi^2 + a(b-1)\phi^3 + \frac{1}{4}\phi^4 + C$$

two minima at $\phi = 0$ and $\phi = 2a$

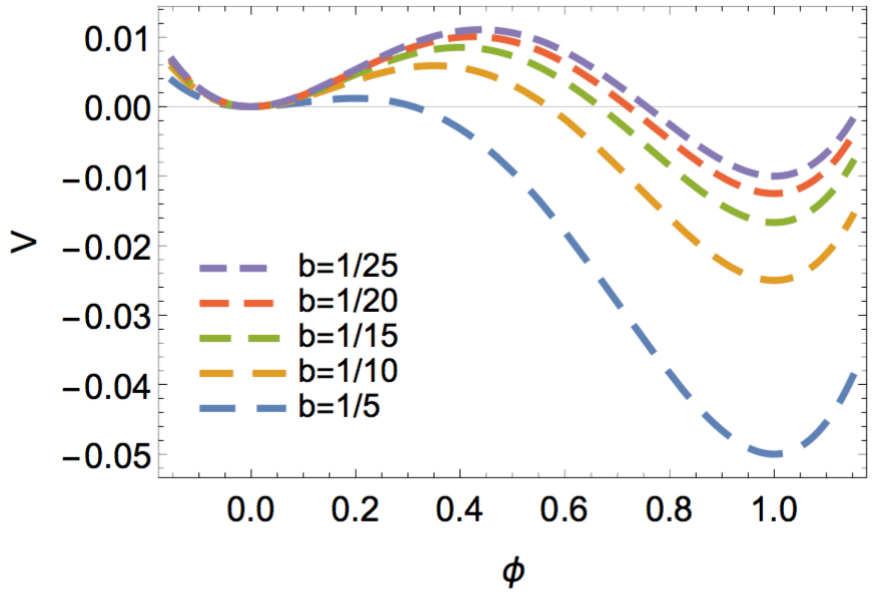

$C = 0$

Figure 1. Our toy model potential for different values of b parameter. In this example vacuum energy vanishes $c = 0$. Different choices of vacuum energy, we will discuss, simply mean adding a constant to the potential.

Transition probability

$$\Gamma = Ae^{-S}$$

$$S_{\text{CDL}} = S[\phi_{\text{CDL}}] - S[\phi_{\text{fv}}]$$

$$S[\phi_{\text{fv}}] = -\frac{24\pi^2}{V_{\text{min}}}, \quad \text{(for dS)}$$
$$S[\phi_{\text{fv}}] = 0, \quad \text{(for Minkowski)}$$

$$ds^2 = d\tau^2 + r(\tau)^2(d\Omega)^2$$

$$S_E = 2\pi^2 \int d\tau \rho^3 \left(\frac{1}{2}\dot{\phi}^2 + V + \frac{1}{2}R \right)$$

$$R = 6\left(\frac{\ddot{\rho}}{\rho} + \left(\frac{\dot{\rho}}{\rho} \right)^2 - \frac{1}{\rho^2} \right) \text{ and } \dot{\phi} = \frac{d\phi}{d\tau}$$

Equations of motion

$$\ddot{\phi} + 3\frac{\dot{\rho}}{\rho}\dot{\phi} = \frac{\partial V}{\partial \phi}$$

$$\dot{\rho} = \sqrt{1 + \frac{\rho^2}{3}\left(\frac{1}{2}\dot{\phi}^2 - V\right)}$$

Boundary conditions

$$\begin{aligned}
\dot{\phi}(0) &= \dot{\phi}(\tau_{\text{end}}) = 0 \\
\rho(0) &= 0 \\
\rho(\tau_{\text{end}}) &= 0, \quad \text{(for dS)} \\
\rho(\tau_{\text{end}}) &= \rho_{\text{end}} \neq 0, \quad \text{(for Minkowski)}
\end{aligned}$$

Hawking-Moss solution

Simpler HM solution S.W. Hawking, I.G. Moss, Phys.Lett. B 110 (1982) describes the probability for a whole spacetime volume to transition simultaneously to the top of the barrier (max) and continue by a classical roll-down:

$$S_{HM} = S_{\max} - S_{fv} =$$
$$= -\frac{24\pi^2(1-\kappa\xi\phi_{\max}^2)^2}{\kappa^2 V_{\max}} + \frac{24\pi^2(1-\kappa\xi\phi_{fv}^2)^2}{\kappa^2 V_{fv}}$$

including the modification coming from ξ

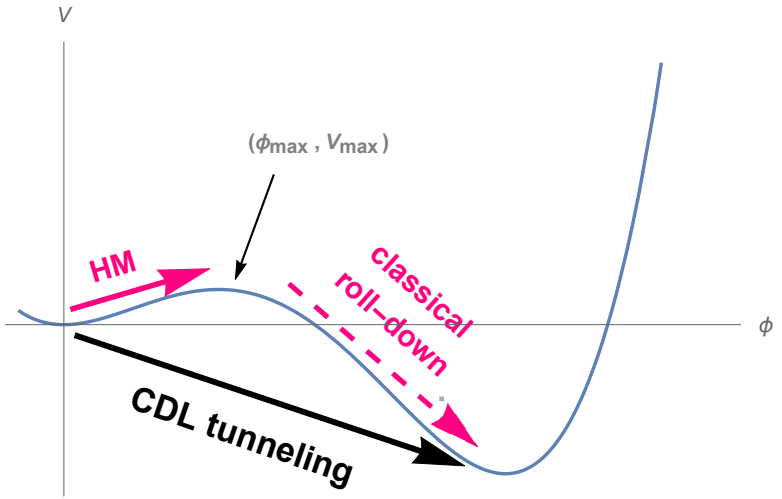

Comparison of the results

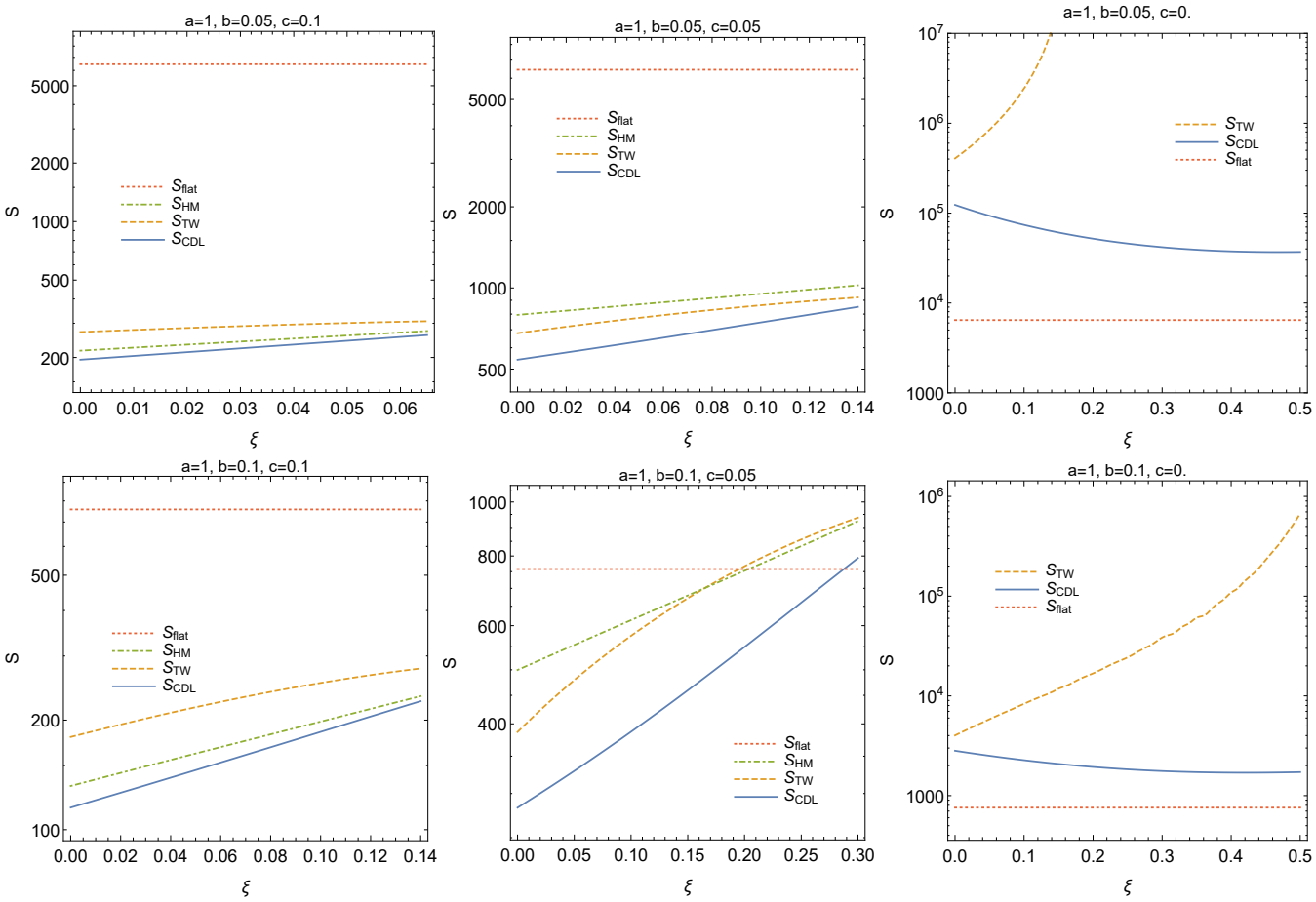

Tunnelling action as a function of non-minimal coupling obtained using four different methods with $c = (0.1, 0.05, c = 0$ (Minkowski)$)$.

Hawking-Moss vs CDL

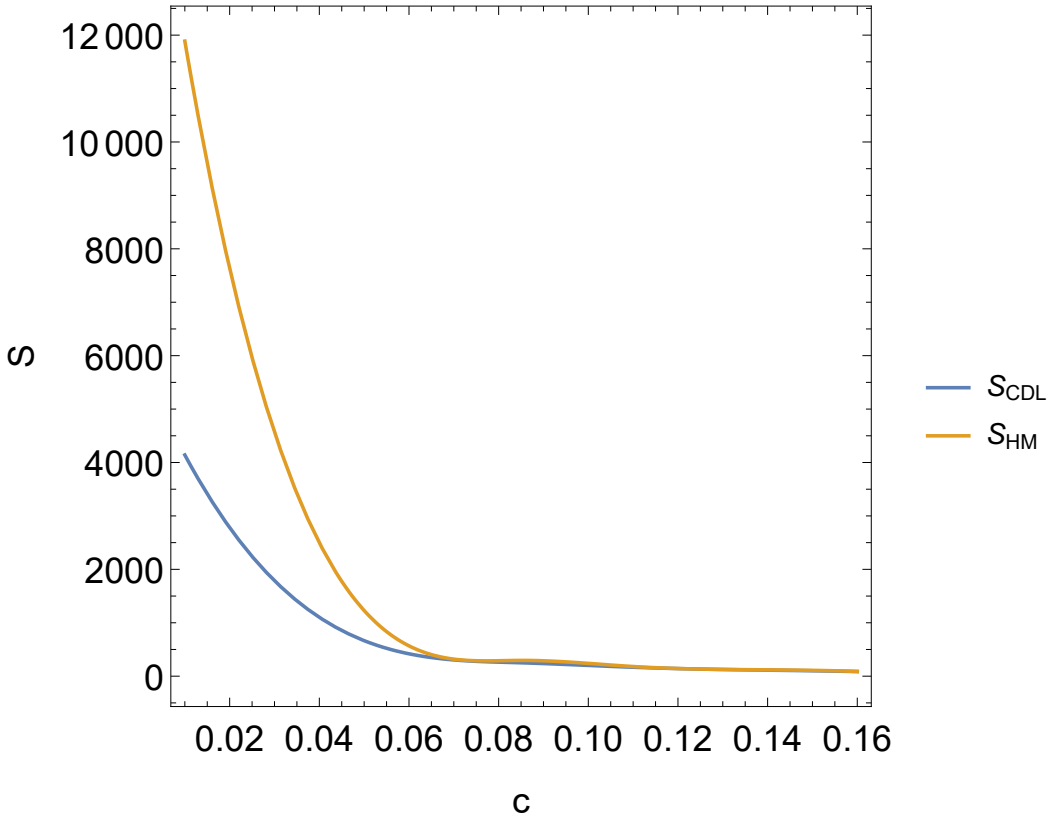

Conclusions CDL

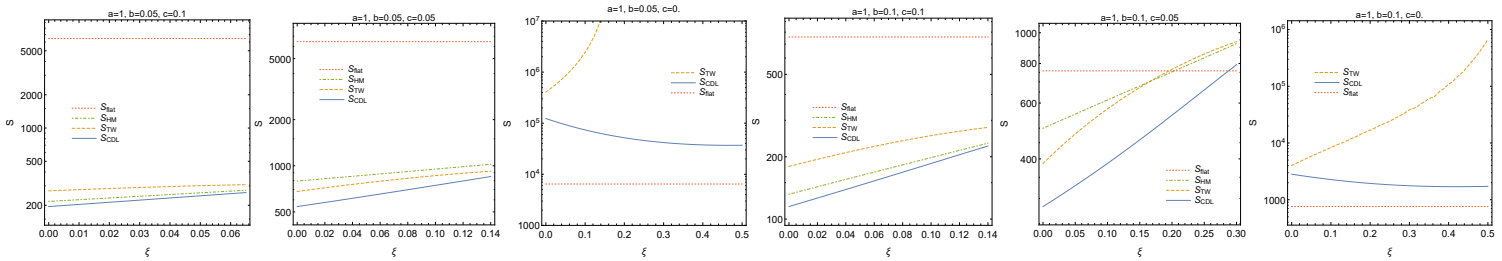

The influence of non-minimal coupling to gravity is very different in cases of Minkowski and dS vacua:

- dS - the decay probability quickly decreases as the coupling grows, vacuum can be made absolutely stable
- Minkowski - effect is much weaker, the decay rate increases for small values, TW approximation works worse significantly overestimating the increase in action due to ξ

Even though TW approximation may not give a precise result in a specific model, the order of magnitude is right (especially in dS case where gravitational correction decreases the stability).

Domain walls and gravitational waves

Network of walls prefers the true vacuum!

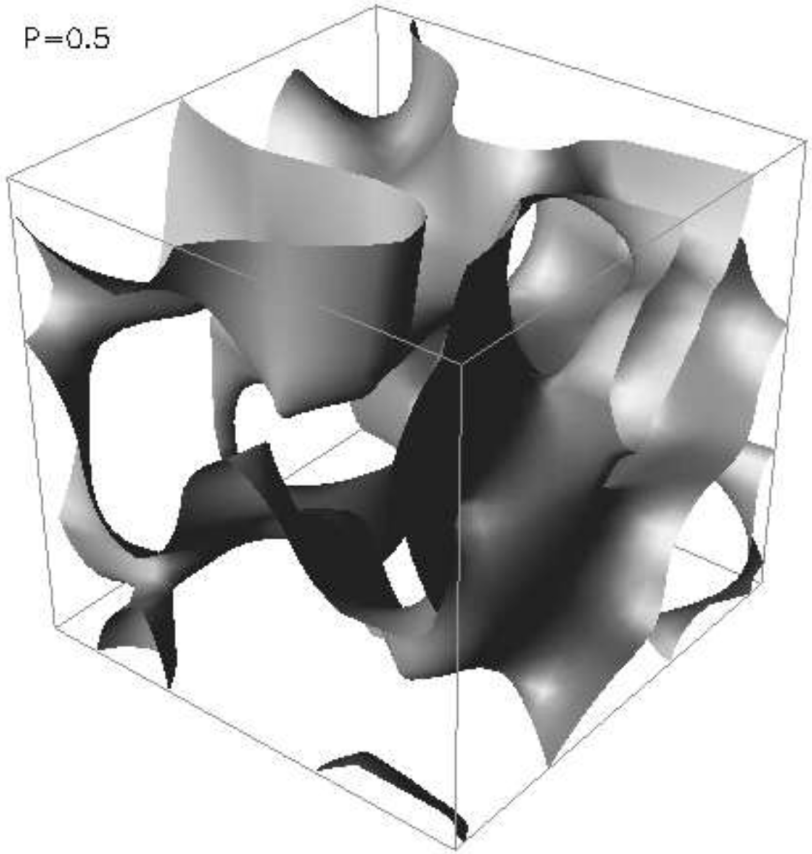

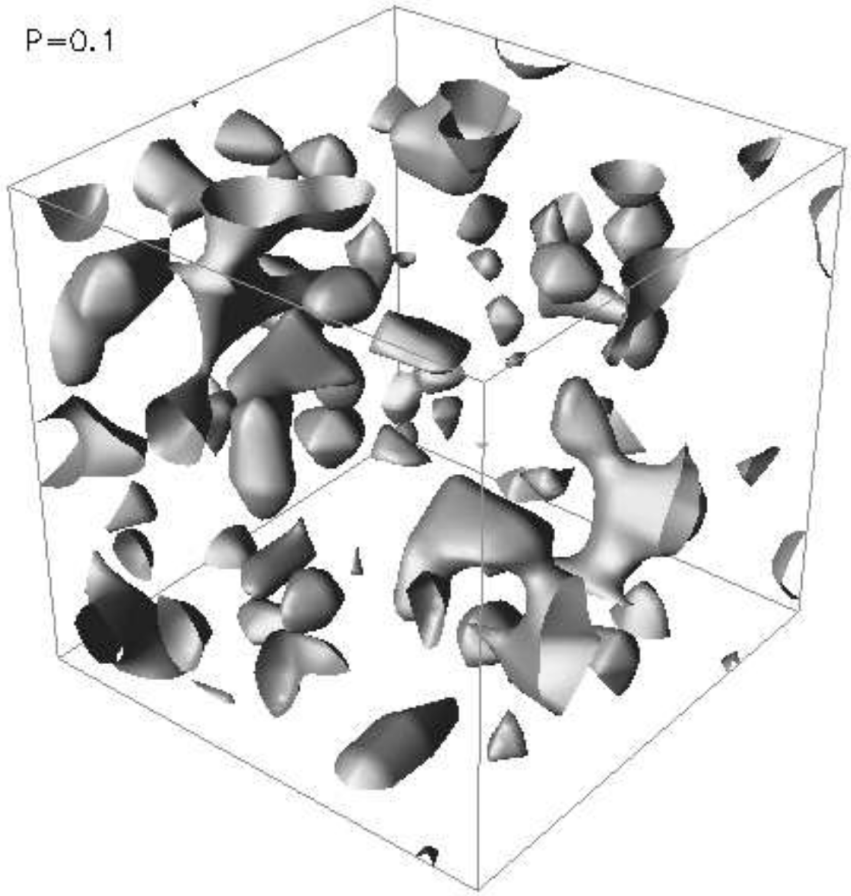

About our simulation

- We modeled the Higgs field with a positive, real scalar ϕ.
- The evolution of ϕ is given by EOM:

$$\frac{\partial^2\phi}{\partial\eta^2} + \frac{\alpha}{\eta}\left(\frac{d\ln a}{d\ln\eta}\right)\frac{\partial\phi}{\partial\eta} - \Delta\phi = -a^\beta\frac{\partial V}{\partial\phi},$$

  with a potential $V(\phi)$ equal to the RG improved potential of the SM Higgs $V_{\mathrm{SM}}(|h|)$.
- The PRS algorithm[2] (with $\alpha = 3$, $\beta = 0$) was used.
- We used the optimization of a time step[3].
- Our simulations were run on a lattice of the size 512^3.

[2] William H. Press, Barbara S. Ryden, and David N. Spergel. "Dynamical Evolution of Domain Walls in an Expanding Universe". In: *Astrophys. J.* 347 (1989), pp. 590–604. DOI: 10.1086/168151.

[3] Z. Lalak, S. Lola, and P. Magnowski. "Dynamics of domain walls for split and runaway potentials". In: *Phys. Rev.* D78 (2008), p. 085020. DOI: 10.1103/PhysRevD.78.085020. arXiv: 0710.1233 [hep-ph].

Initial conditions

Following the general considerations[4] we assumed that the initial distribution of field strength is given by probability distribution:

$$P(h) = \frac{1}{\sqrt{2\pi}\sigma_I} e^{-\frac{(h-\theta)^2}{2\sigma_I^2}} \quad \sigma_I \sim \frac{\sqrt{N} H_I}{2\pi}$$

We considered various combinations of values of σ and θ in order to cover the set of initial conditions which can be predicted by models of the early Universe.

Our simulations were initialized at different conformal times η_{start} ranging from $10^{-14}\ \mathrm{GeV}^{-1}$ to $10^{-10}\ \mathrm{GeV}^{-1}$.

[4] Z. Lalak et al. "Large scale structure from biased nonequilibrium phase transitions: Percolation theory picture". In: *Nucl. Phys.* B434 (1995), pp. 675–696. DOI: 10.1016/0550-3213(94)00557-U. arXiv: hep-ph/9404218 [hep-ph].

Dependence on the initialization time

The decay of domain walls ending in the state without the EW vacuum is possible even for the initial configuration with a slight dominance of the EW vacuum.

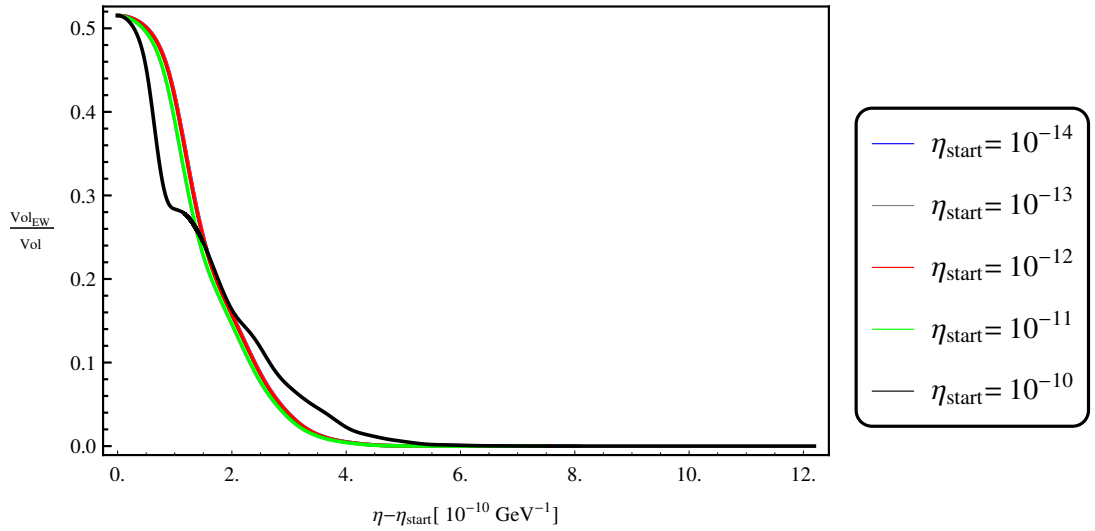

Figure: The fraction $\frac{Vol_{EW}}{Vol}$ as a function of conformal time η for different initialization times η_{start}.

Dependence on standard deviation σ

We investigated the initial conditions satisfying $\theta + \sigma = v_{max}$, where v_{max} is position of the local maximum of the potential. In this case the evolution of networks displays the weak dependence on the value of σ and for all simulations the final state is the EW vacuum.

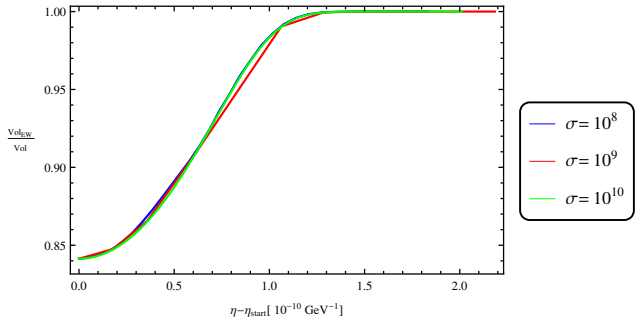

Figure: The fraction $\frac{Vol_{EW}}{Vol}$ as a function of conformal time η for initialization time $\eta_{start} = 10^{-13}$ GeV^{-1} and different values of standard deviation σ.

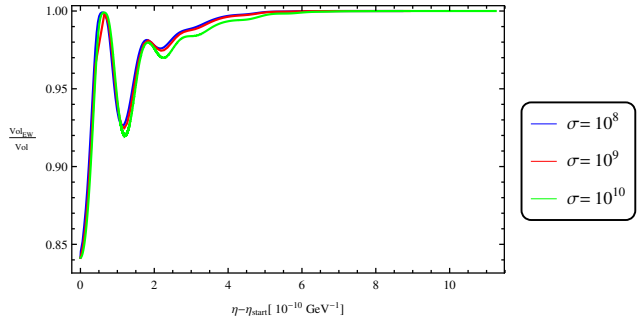

Figure: The fraction $\frac{Vol_{EW}}{Vol}$ as a function of conformal time η for initialization time $\eta_{start} = 10^{-10}$ GeV^{-1} and different values of standard deviation σ.

Higgs domain walls after reheating

Higgs domain walls after reheating

- After reheating the early Universe was very hot and dense and it was better described that time by the thermal state with temperature T, than by the vacuum state.
- The dynamics of Higgs domain walls in the background of this thermal state could be different than in the vacuum state.
- The evolution of the domain walls in the cooling down Universe can be determined reliably only in lattice simulations.

Thermal effective potential

$$V_{\text{eff}}(h,T) = \frac{1}{2}m^2h^2 + \frac{1}{4}\lambda h^4 + \sum_{i=\varphi,\chi,W,Z,t} \frac{1}{2}n_i T \sum_{n=-\infty}^{\infty} \int \frac{d^3\vec{k}}{(2\pi)^3} \log\left[\vec{k}^2 + {\omega_n}^2 + {m_i}^2(\phi)\right]$$

$$\begin{aligned}
{m_h}^2(\phi) &= m^2 + 3\lambda h^2, \\
{m_{\chi_i}}^2(\phi) &= m^2 + \lambda h^2, \\
{m_W}^2(\phi) &= \frac{g^2}{4} hi^2, \\
{m_Z}^2(\phi) &= \frac{g^2 + g'^2}{4} h^2, \\
{m_t}^2(\phi) &= \frac{{y_t}^2}{2} h^2,
\end{aligned}$$

$$\begin{aligned}
V_{\text{SM}}(h,T) = \frac{1}{2}m^2h^2 + \frac{1}{4}\lambda h^4 &+ \sum_{i=\varphi,\chi,W,Z,t} n_i \frac{{m_i}^4(h)}{64\pi^2}\left[\log\frac{{m_i}^2(h)}{\mu^2} - C_i\right] \\
&+ \sum_{i=\varphi,\chi,W,Z} \frac{n_i T^4}{2\pi^2} J_b\left(\frac{{m_i}^2(h)}{T^2}\right) + \frac{n_t T^4}{2\pi^2} J_f\left(\frac{{m_t}^2(h)}{T^2}\right) \\
&+ \sum_{i=\varphi,\chi,W,Z,\gamma} \frac{\bar{n}_i T}{12\pi}\left[{m_i}^3(h) - \left({m_i}^2(h) + \Pi_i(T)\right)^{\frac{3}{2}}\right],
\end{aligned}$$

$$J_{b/f}(x) := \int_0^\infty dk k^2 \log\left[1 \mp e^{-\sqrt{k^2+x}}\right]$$

Removal of IR divergencies - resumption of daisy diagrams
- shift by Debye masses

$$\Pi_{\varphi,\chi_i}(T) = \frac{T^2}{4{h_{EW}}^2}({m_\varphi}^2(h) + 2{m_W}^2(h) + {m_Z}^2(h) + 2{m_t}^2(h)),$$

$$\Pi_W(T) = \frac{22}{3}\frac{{m_W}^2(h)}{{h_{EW}}^2}T^2,$$

$${m_{Z/\gamma}}^2 + \Pi_{Z/\gamma}(T)$$

$$\begin{pmatrix} \frac{1}{4}g^2h^2 + \frac{11}{6}g^2T^2 & -\frac{1}{4}g'^2g^2h^2 \\ -\frac{1}{4}g'^2g^2h^2 & \frac{1}{4}g'^2h^2 + \frac{11}{6}g^2T^2 \end{pmatrix}$$

Position of the local maximum

Figure : The position h_{max} of the local maximum separating two minima of the RG improved effective potential as a function of the temperature of thermal bath T.

Width of Higgs domain walls

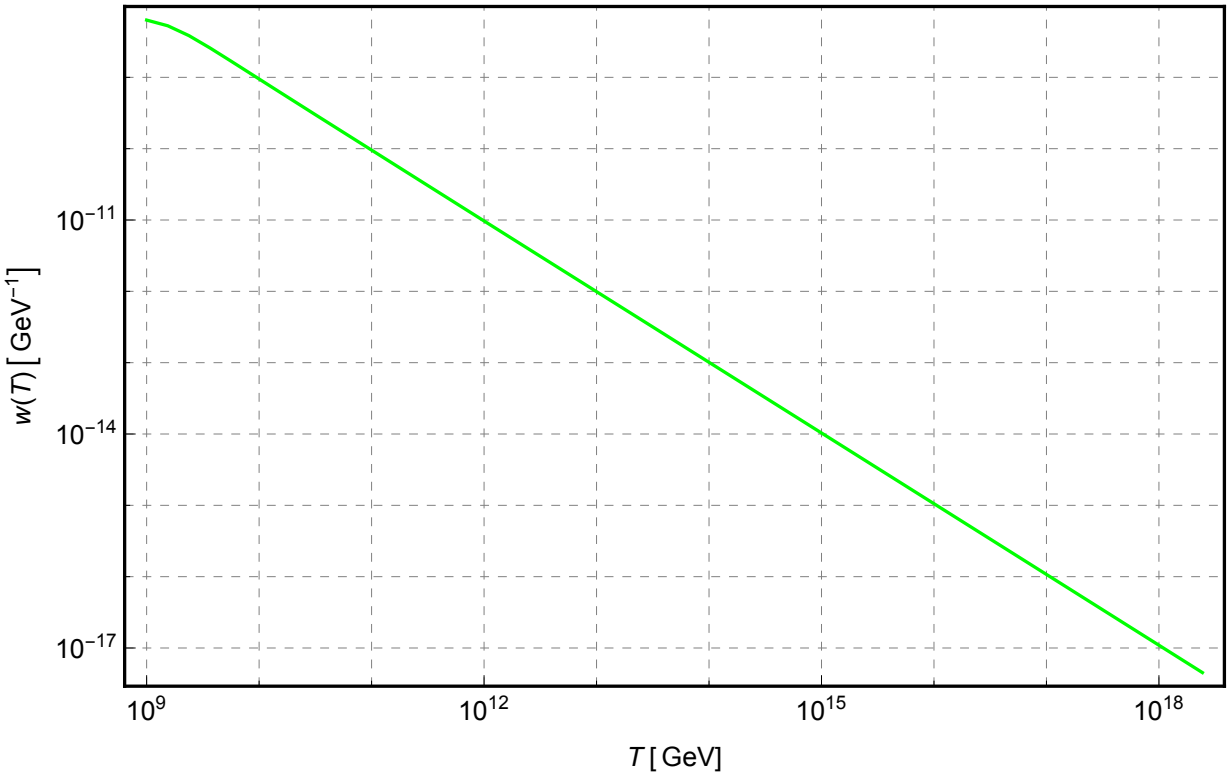

Figure : The width of domain walls w as a function of the temperature T.

Bounds on the standard deviation σ

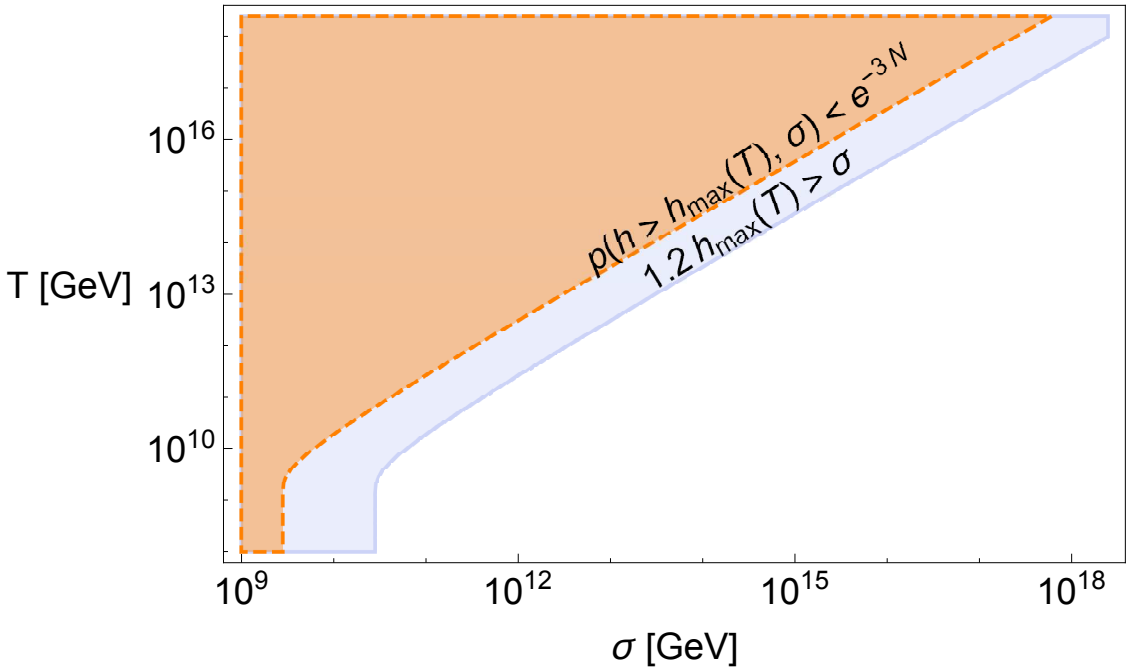

Figure : Maximal value of the standard deviation σ_I of initial distribution for given temperature T.

Bounds on the reheating temperature T_{RH}

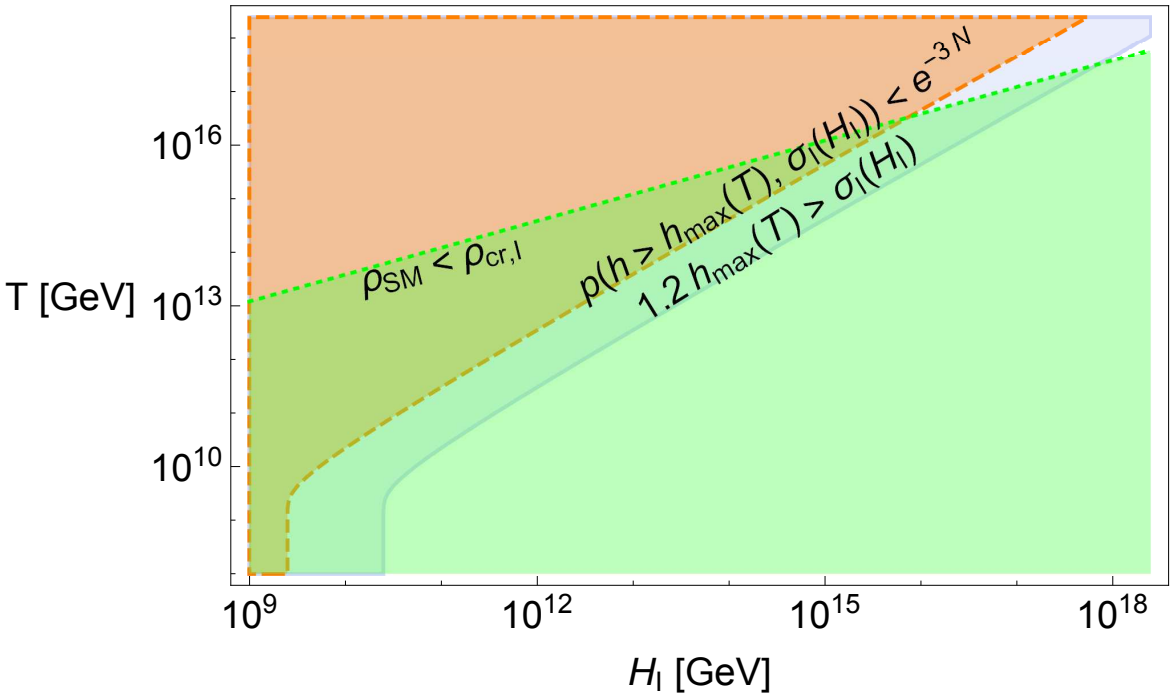

Figure : Maximal value of the reheating temperature from inflation with Hubble parameter value H_I.

Evolution in the thermal background

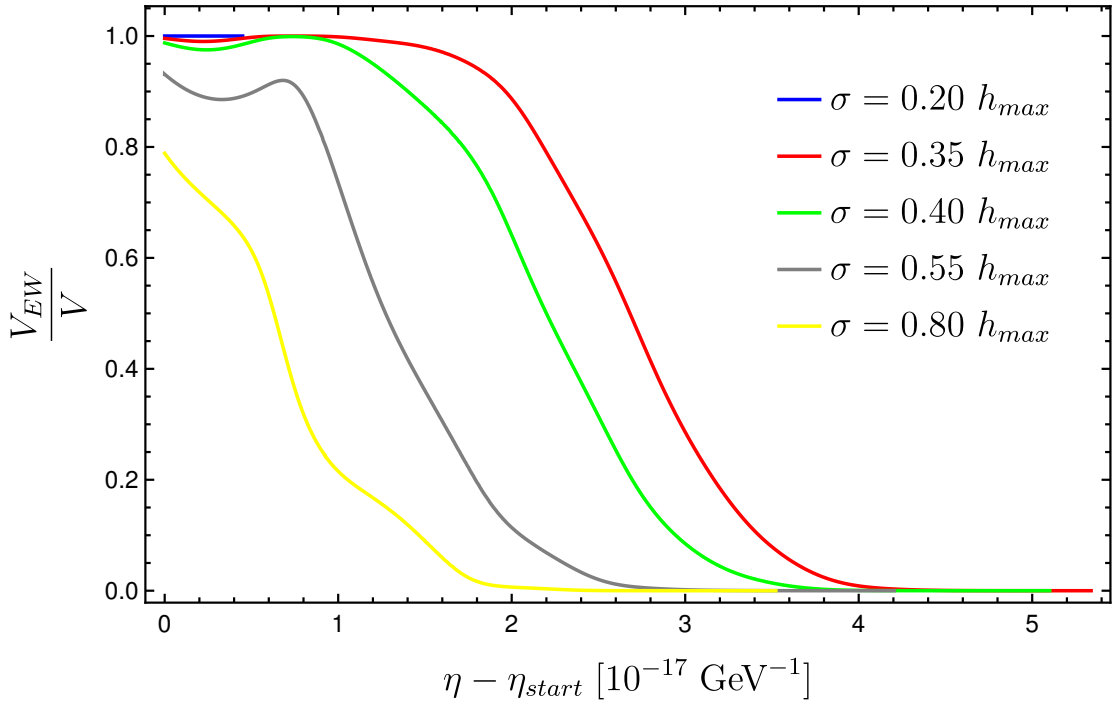

Figure : The fraction $\frac{V_{EW}}{V}$ as a function of conformal time η for values of standard deviation σ of initialization distribution.

Summary - thermal bath

- SM thermal corrections to the effective potential enlarge the basin of attraction of the EWSB vacuum
- Higgs domain walls in the thermal bath are highly unstable

Gravitational waves from domain walls

Gravitational waves from domain walls

Energy density generated by one mode $\varrho_{gw}(\eta, k)$ can be expressed as:

$$\varrho_{gw}(\eta,k) = \frac{1}{16\pi^3 {M_{Pl}}^2 a(\eta)^4 V} \sum_{i,j} \left[\left| \int_{\eta_i}^{\eta_f} d\eta' \cos\left(|k|\left(\eta-\eta'\right)\right) a(\eta') \widehat{T^{TT}}_{ij}(\eta', k) \right|^2 \right.$$
$$\left. + \left| \int_{\eta_i}^{\eta_f} d\eta' \sin\left(|k|\left(\eta-\eta'\right)\right) a(\eta') \widehat{T^{TT}}_{ij}(\eta', k) \right|^2 \right],$$

after redshift

$$\frac{d\rho_{gw}}{d\log|k|}(\eta_0, k) = (1+z_{EQ})^{-4} \frac{a(\eta_{dec})^4}{a(\eta_{EQ})^4} \frac{d\rho_{gw}}{d\log|k|}(\eta_{dec}, k),$$

$$f_0 = \frac{a(\eta_{dec})}{a(\eta_0)} \frac{k}{2\pi} = 5.07 \times 10^6 \left(\frac{10^{19}\,\frac{\mathrm{eV}}{\hbar}}{H_{dec}} \right)^{\frac{1}{2}} \left(\frac{k}{10^{10}\,\frac{\mathrm{GeV}}{\hbar c}} \right) \mathrm{Hz}.$$

Expectations:

N. Kitajima and F. Takahashi, *Gravitational waves from Higgs domain walls*, *Phys. Lett.* **B745** (2015) 112–117, [1502.03725].

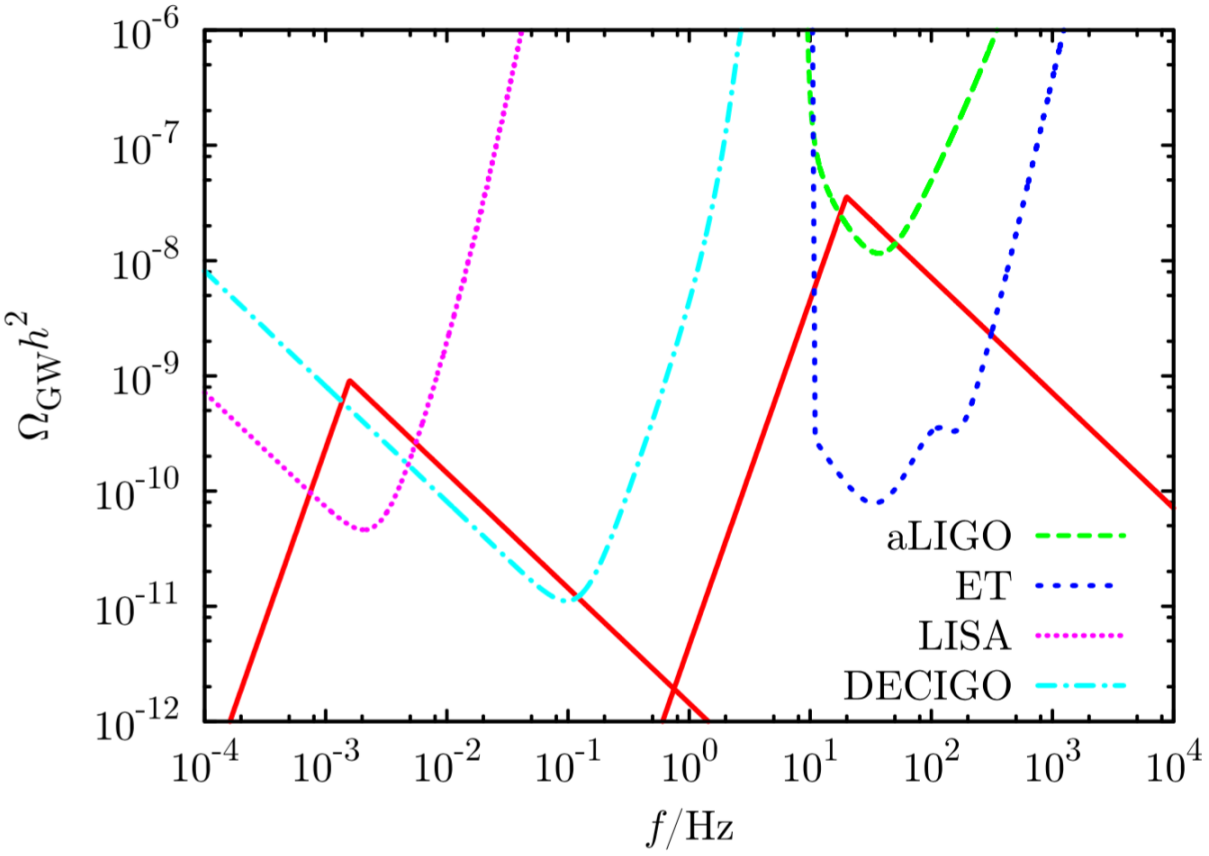

Fig. 3. The typical spectrum of the gravitational waves is shown by the solid (red) lines. We have taken $\varphi_f = 2 \times 10^9$ GeV and $(V_f/V_{\rm max})^{1/4} = 5 \times 10^{-5}$ for the left line and $\varphi_f = 2 \times 10^{12}$ GeV and $(V_f/V_{\rm max})^{1/4} = 10^{-3}$ for the right line.

Numerical simulations:

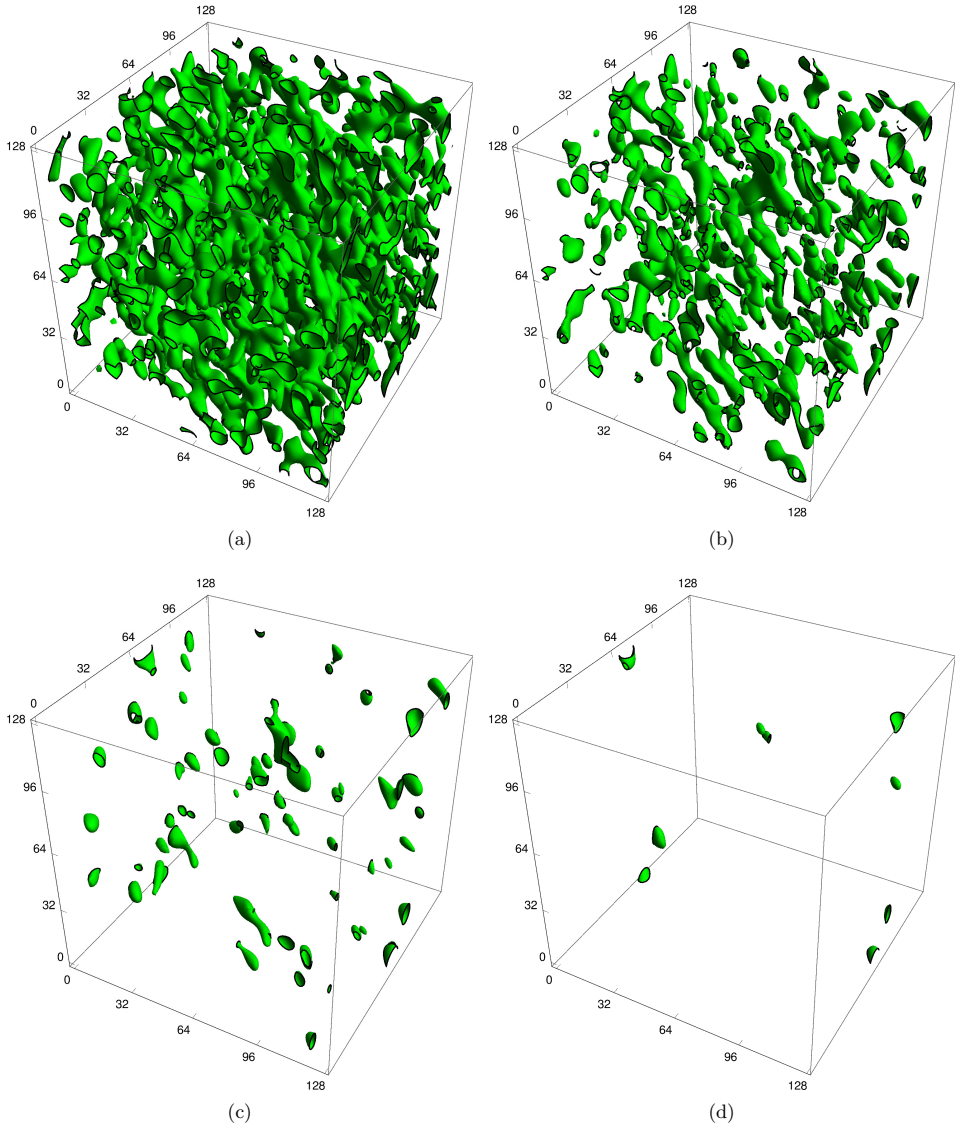

Figure 11: **Visualization of the isosurface of the field strength ϕ corresponding the value v_{max} at four different conformal times: $\eta = 10^{-9}$ GeV^{-1} (a) and $\eta = 1.2 \times 10^{-9}$ GeV^{-1} (b), $\eta = 1.3 \times 10^{-9}$ GeV^{-1} (c), $\eta = 1.4 \times 10^{-9}$ GeV^{-1}(d). Lengths are given in units of the lattice spacing i.e. 10^{-10} GeV^{-1}.**

Spectrum of GWs after emission

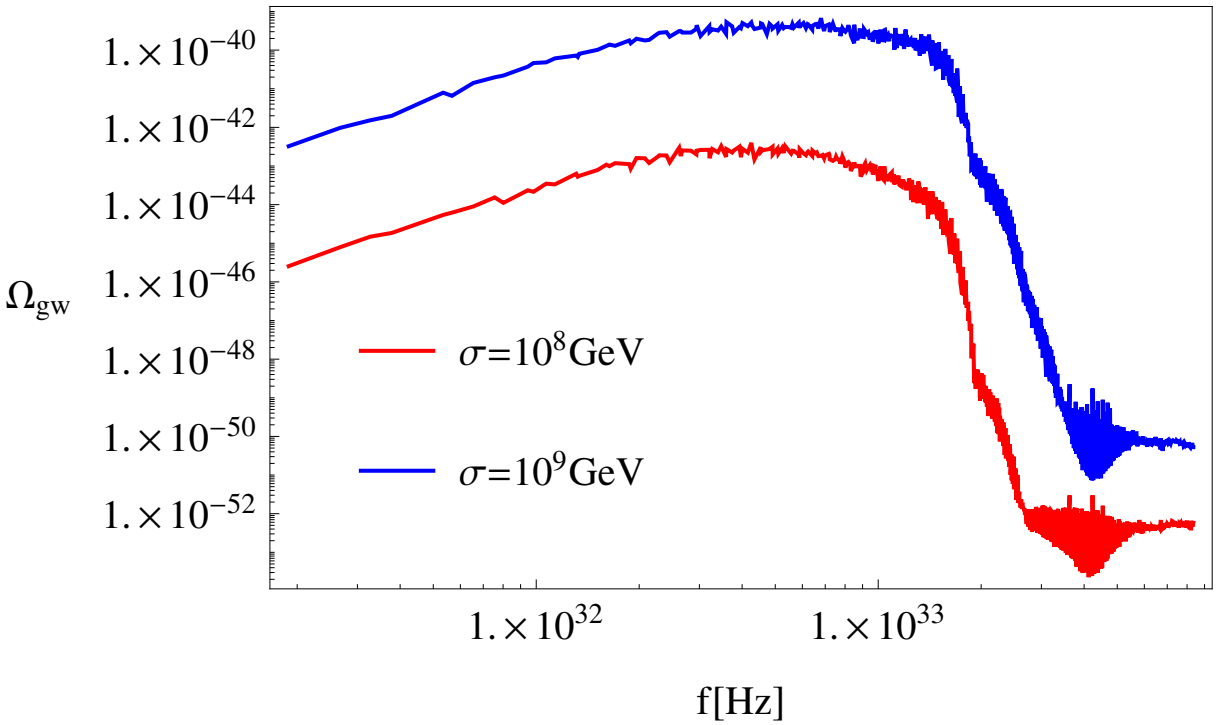

Figure: Spectrum of gravitational waves Ω_{gw} emitted from SM domain walls at the time of the decay.

Present spectrum of GWs

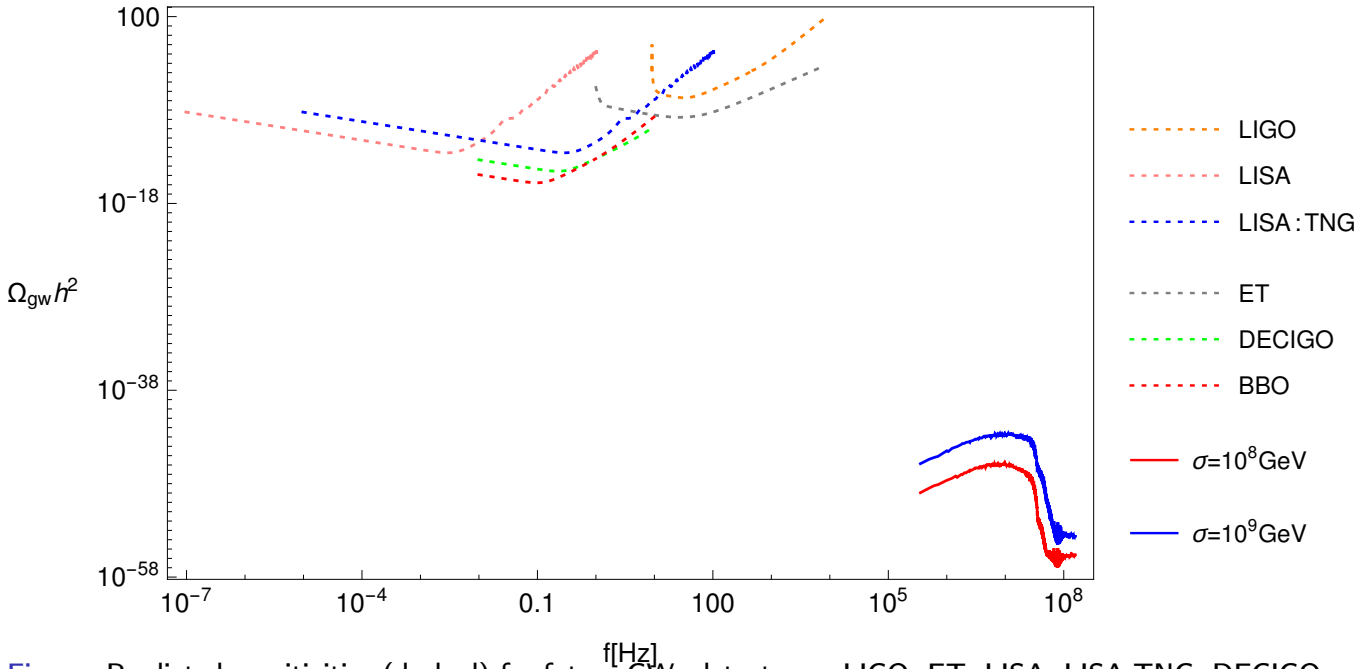

Figure: Predicted sensitivities (dashed) for future GWs detectors: aLIGO, ET, LISA, LISA:TNG, DECIGO and BBO compared with the spectrum of GWs (solid) calculated in lattice simulations for the initial values of $\sigma = 10^8,\ 10^9$ GeV and the standard cosmology.

New Physics and domain walls

New physics $\delta V_{SM}^{\Lambda}(h) = \frac{\lambda_6}{6!}\frac{h^6}{\Lambda_{NP}^2}$

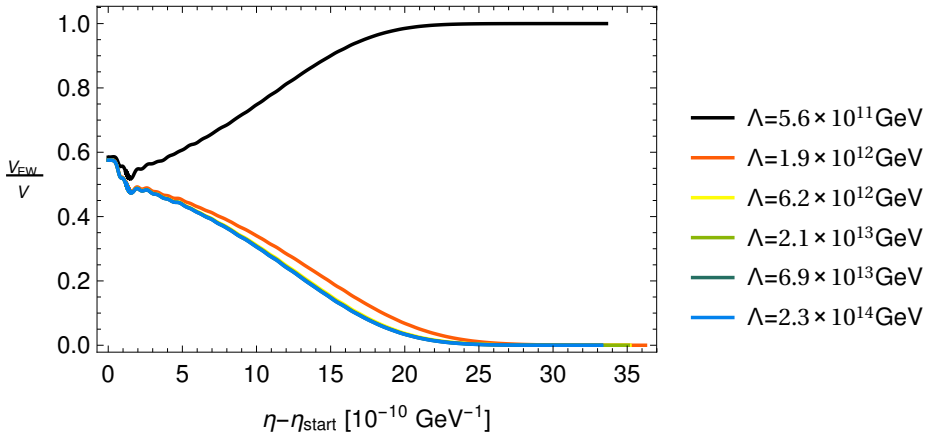

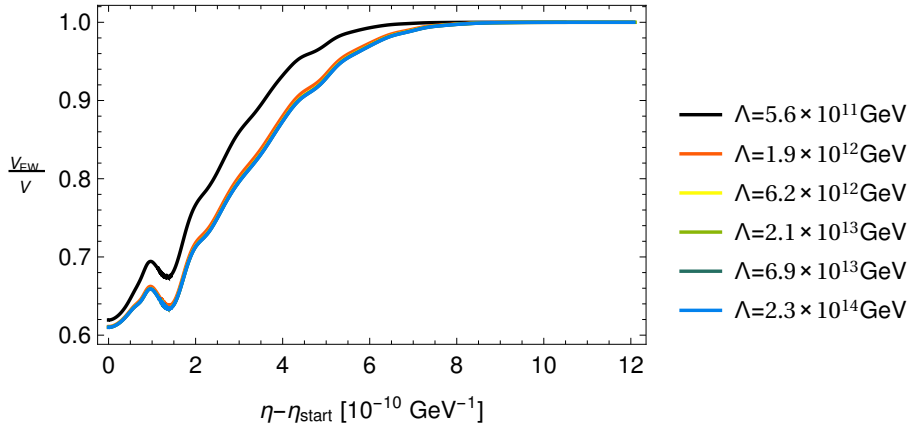

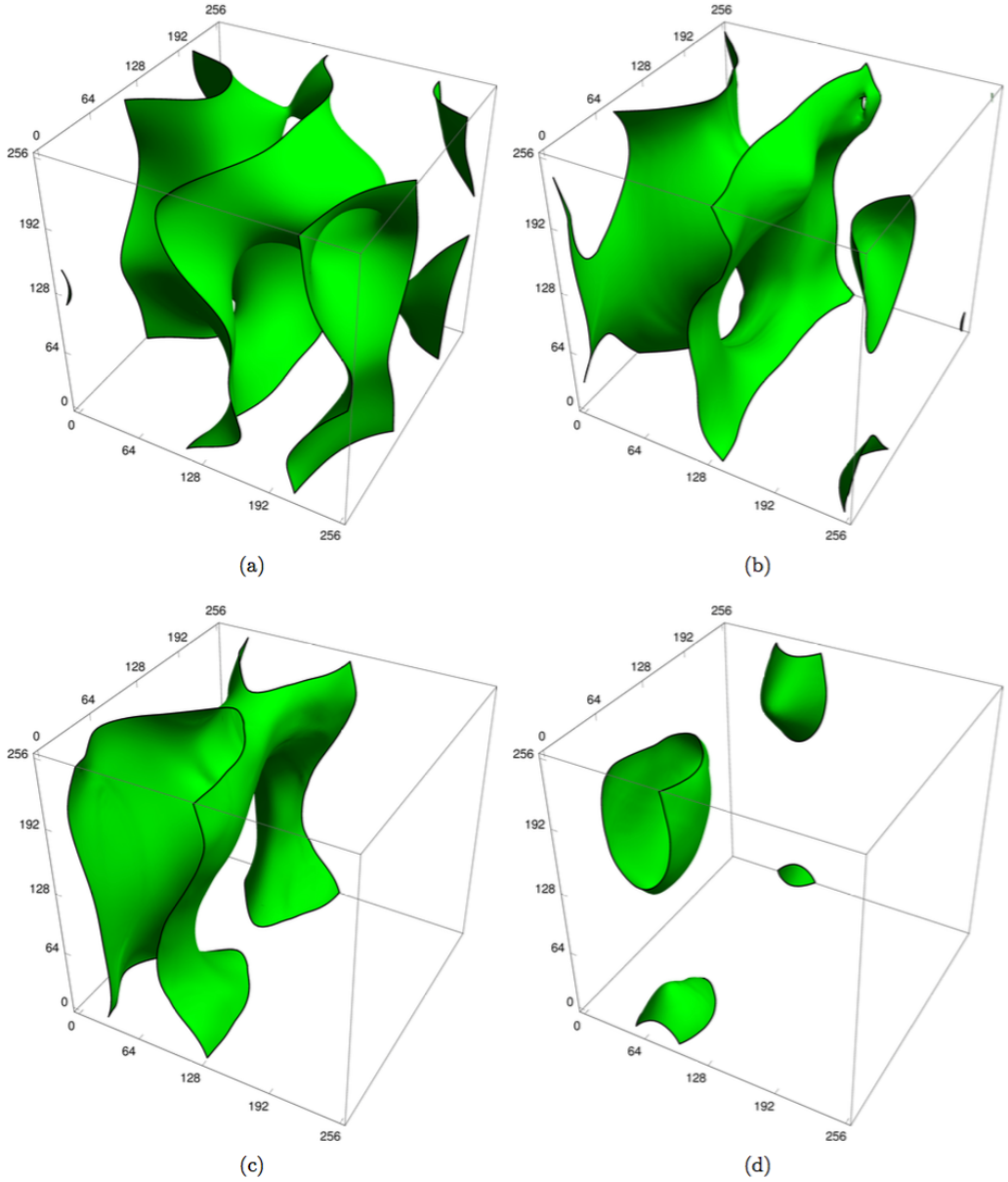

Figure 10: Visualization of the isosurface of the field strength ϕ corresponding to the value h_{max} at four different conformal times: $\eta = 1.41\times10^{-8}$ GeV^{-8} (a) and $\eta = 2.11\times10^{-8}$ GeV^{-1} (b), $\eta = 2.51 \times 10^{-8}$ GeV^{-1} (c), $\eta = 3.02 \times 10^{-8}$ GeV^{-1}(d). Lengths are given in units of the lattice spacing i.e. 10^{-10} GeV^{-1}.

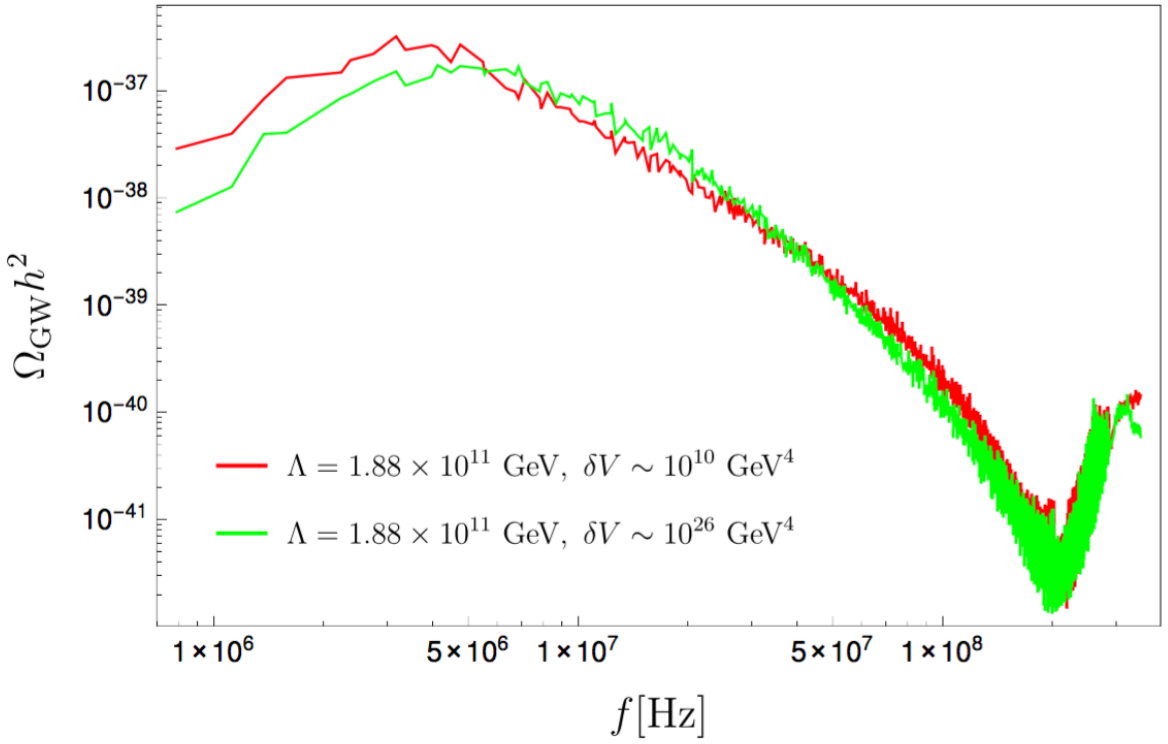

Figure 11: Present day spectrum of gravitational waves Ω_{gw} emitted from Higgs domain walls in the case of the Higgs potential with nearly degenerate minima with the difference in values of potential in minima of the order of $\delta V \sim 10^{10}$ GeV^4 (red) and $\delta V \sim 10^{26}$ GeV^4 (green).

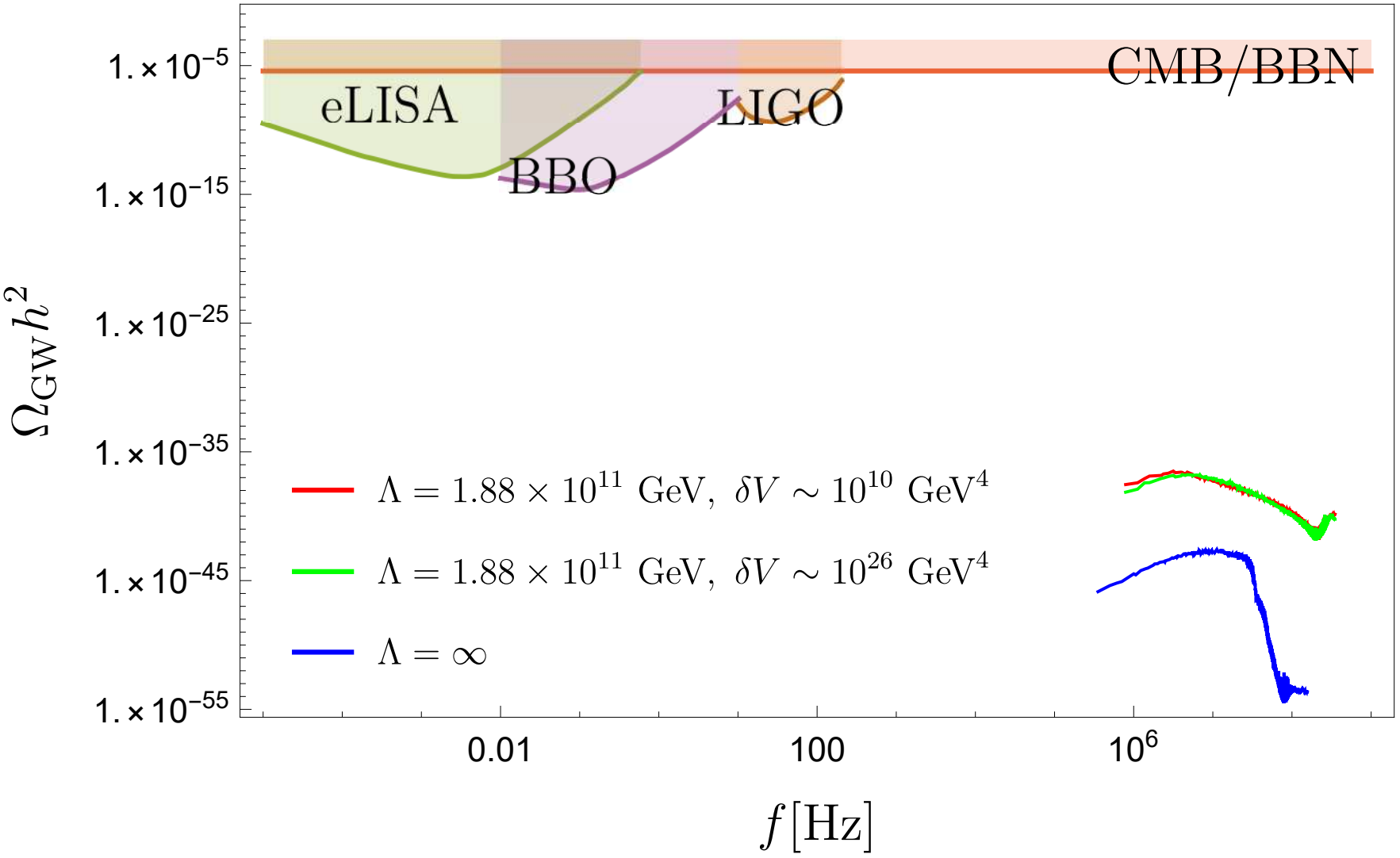
$1.\times10^{-5}$
$1.\times10^{-15}$
$1.\times10^{-25}$
$1.\times10^{-35}$
$1.\times10^{-45}$
$1.\times10^{-55}$
$\Omega_{\rm GW}h^2$
eLISA
BBO
LIGO
CMB/BBN
$\Lambda = 1.88\times10^{11}$ GeV, $\delta V \sim 10^{10}$ GeV^4
$\Lambda = 1.88\times10^{11}$ GeV, $\delta V \sim 10^{26}$ GeV^4
$\Lambda = \infty$
0.01
100
10^6
f [Hz]

Summary I

1. New Physics at scales higher than 10^{13} GeV does not influence Higgsa domain walls.
2. Networks of domain walls initialized with $\sigma < 3.25 \times 10^{10}$ GeV decay to the EWSB vacuum.
3. For lower values of the scale Λ lifetimes of Higgs domain walls are still short and smaller than 10^{-8} $\frac{\hbar}{\mathrm{GeV}}$ for generic inital configurations.
4. Thermal corrections to the effective potential stabilize the Higgs field by enlarging the basing of attraction of EWSB vacuum.
5. Higgs domain walls in the thermal background are highly unstable.
6. Gravitational waves produced from generic initial configurations are too weak to be detected in the planned detectors.

Summary II

- SM vacuum can be stabilized by higher order operators if they appear at suffciently low energy scale $10^{10} - 10^{11}\,\mathrm{GeV}$
- SM vacuum lifetime can be dramatically shortened by higher order operators for any suppression scale
- Beyond the leading order one needs to define proper expansion of the action to demonstrate perturbatively the cancellation of gauge-dependent contributions to the lifetime of the EW vacuum. In the abelian Higgs model such a procedure can be carried out at the level of the renormalized effective action
- Peoperties of the electroweak vacuum - critical temperature and lifetime - can be modified by a fast expansion of the gravitational background
- Tunneling from Minkowski suppressed by gravity but tunnelling from dS enhanced by CDL bounces
- Decaying networks of domain walls produce a signal in the form of gravitational waves - too weak to be detected anytime soon - if a signal is detected then either fine-tuning or non-standard cosmology have occurred